

## Stress-strain behaviour analysis of Middle Polish glacial tills from Warsaw (Poland) based on the interpretation of advanced field and laboratory tests

ANNA BĄKOWSKA, PAWEŁ DOBAK, IRENEUSZ GAWRIUCZENKOW, KAMIL KIEŁBASIŃSKI, TOMASZ SZCZEPAŃSKI, JERZY TRZCIŃSKI, EMILIA WÓJCIK\* and PIOTR ZAWRZYKRAJ

*Institute of Hydrogeology and Engineering Geology, Faculty of Geology, University of Warsaw, Al. Żwirki i Wigury 93, 02-089 Warszawa, Poland. 02-089 Warszawa, Poland. \* E-mail: wojcike@uw.edu.pl*

### ABSTRACT:

Bąkowska, A., Dobak, P., Gawriuczenkow, I., Kielbasiński, K., Szczepański, T., Trzciniński, J., Wójcik, E. and Zawrzykraj, P. 2016. Stress-strain behaviour analysis of Middle Polish glacial tills from Warsaw (Poland) based on the interpretation of advanced field and laboratory tests. *Acta Geologica Polonica*, **66** (3), 561–585. Warszawa.

The selected parameters of the Wartanian and Odranian tills, with relation to their spatial occurrence, grain size distribution, mineralogical composition, matric suction and other physical characteristics, are presented. The assessment of the lithogenesis and stress history on the microstructure is attempted. The comparison of the compression and permeability characteristics from field and laboratory tests has been performed. Laboratory consolidation tests carried out with up to 20MPa vertical stress, revealed two yield stress values, one in the range of a couple hundreds kPa, the other in the range of a couple thousands kPa. Based on those results, the reliability of the soil preconsolidation assessment, with the use of the two different methods is discussed. The aspect of the triaxial strength reduction under the dynamic loading of diverse frequency and amplitude is raised. The research results depict a variety of possible geological-engineering characteristics, under the divergent constraints scenarios, of compression or strength weakening origin. The effects of the specialized research program will widen the possibilities of physio-mechanical and structural characterization of soils for geological-engineering purposes.

**Key words:** Glacial tills; Warsaw; Compressibility; Strength; Advanced tests.

### INTRODUCTION

The determination of the characteristic properties of glacial soils is difficult. The proof of this may be seen among the discrepancies between field and laboratory test results documented in the engineering-geological publications referring to regional geological conditions. Test results obtained for glacial tills in Warsaw confirm this variability as wide ranges of values and various distributions are observed. The test results, collected for years, originate from data sets obtained for

different purposes, such as spatial management (Frankowski and Wysokiński 2000), underground construction (Pinińska and Dobak 1987) and geodynamical problems (Kaczmarek and Dobak 2015; Kaczyński *et al.* 2008b; Bąkowska *et al.* 2010). At the same time the progress in methods of determining strength, deformation and permeability parameters creates additional difficulties in comparing the results obtained at different times using various methodologies.

These difficulties in data interpretation and in defining reliable characteristics by derived values rec-

ommended in Eurocode 7, justify the implementation of a research program which endeavours to collect comparative experiences based on a wide spectrum of modern field and laboratory tests. This allows the evaluation of the variability of the soil properties through various test methods, their interpretation and geological conditions of soil deposition.

## GEOLOGICAL SITUATION OF THE AREA ANALYZED

The research presented in this paper refers to glacial tills of the Middle Polish Glaciations occurring down to a depth of 25 m (the typical zone of soil-structure interaction for most buildings and infrastructure). This soil is typical for an area of glacial plateau of the north-eastern part of the Ursynów district of the town of Warsaw. From the geomorphological point of view this area is one of the Warsaw Plains (Kondracki 1998) classified as a denudation plateau. In the Warsaw area the additional unit, distinguished as the so-called “Warsaw hump”, formed by glacial ice sheets of Middle Polish Glaciations (Odranian and Wartanian), is distinguished. Such ge-

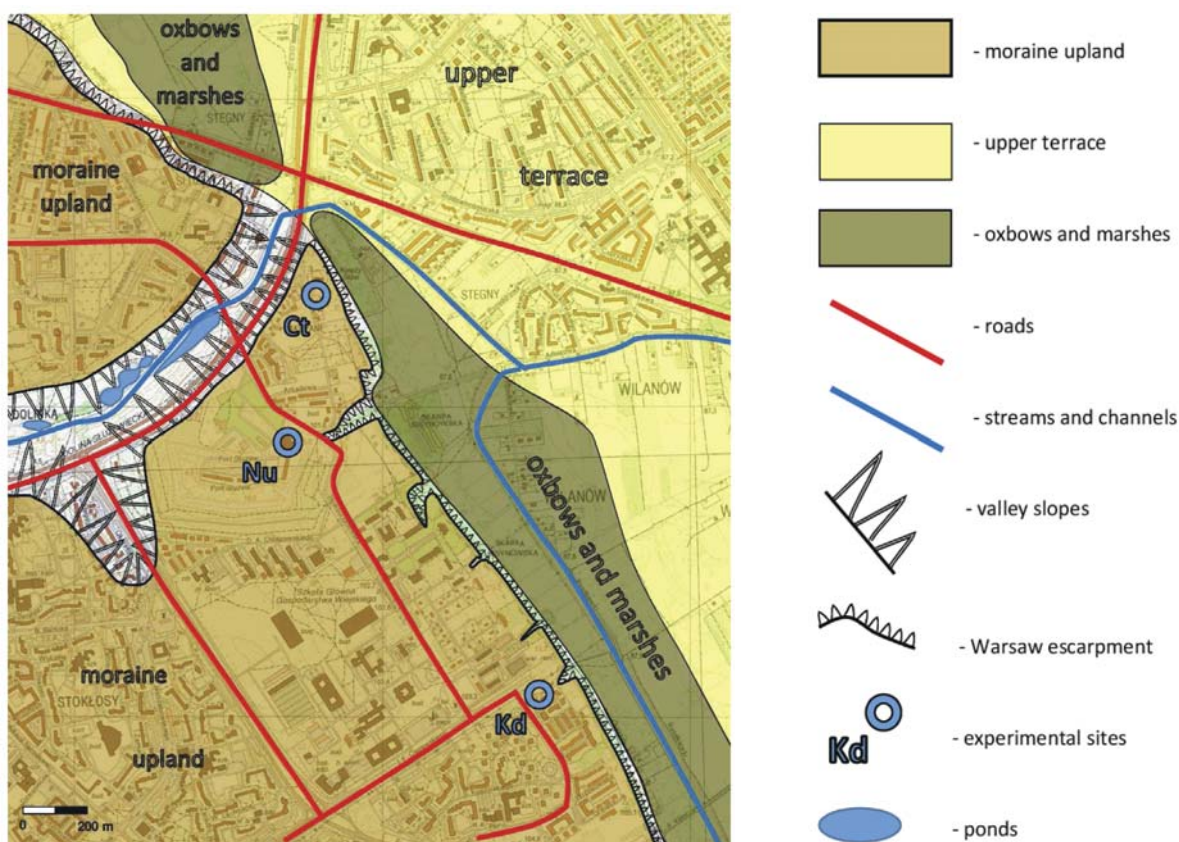
omorphological form descends to the valley of the Vistula River as a steep slope.

The research was carried out at 3 test sites located in the proximity to the edge of the moraine upland (Text-fig. 1). These are:

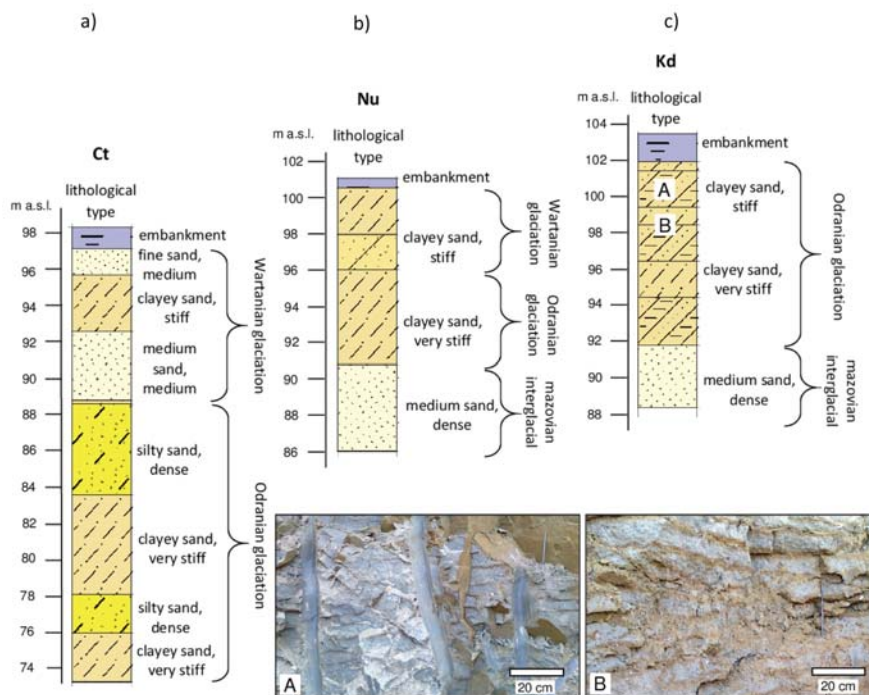
- St. Catherine Church (symbol **Ct**), boreholes Gr1 and Gr1a
- Kiedacza Street (symbol **Kd**), located directly at the slope, borehole Gr2
- Nowoursynowska Street (symbol **Nu**), borehole Gr3

The relief of the upland was formed during the deglaciation of the last glacier in this area (Wartanian glaciation) and its subsequent denudation and erosion. There are significant differences in the lithology at the **Ct** site and at the other two (**Nu** and **Kd**).

The most complex lithology was observed at the St. Catherine Church site (**Ct**) (Text-fig. 2a). This is due to the nature of deglaciation processes. The site is situated at the junction of the Służewiecki Stream with the Vistula River. During the deglaciation of the Odranian glacier, blocks of dead ice were probably present in the place of the present valleys. Their melting led to the formation of kame-type hills, with the accumulation of closely transported sediments. These de-



Text-fig. 1. Geological situation of studied area



Text-fig. 2. Lithological profiles of the studied fields; Ct - St. Katarzyna Church; Nu - Nowoursynowska Street; Kd - Kiedacza Street

posits are: sands, clayey sands and clayey laminae. During the next, Wartanian glaciation, these deposits were covered by c. 6 m thick glacial tills (sandy clay or sandy silty clay) and clayey sands.

At Kiedacza Street test site (**Kd**) (Text-fig. 2b) and Nowoursynowska Street (**Nu**) (Text-fig. 2c) the lithological profiles are typical for southern Warsaw. Fluvio-glacial sands are covered by glacial deposits, associated with the Middle Polish Glaciation. Their thickness varies from 10 (**Kd** site) to 11.60 m (**Nu** site). The sediments of the Wartanian glaciation are thinner, c. 3–6 m, which is the typical thickness in Warsaw. These are sands and gravels with clay and sandy clays. In some places these deposits were removed during levelling works (borehole Gr2) with the result that only Odranian-age soils are present. It should be emphasized that the boundary between the Wartanian and Odranian tills, representing the Middle Polish Glaciation Period, is not clear. This is due to the general lack of fluvio-glacial sediments or soil horizons separating both tills.

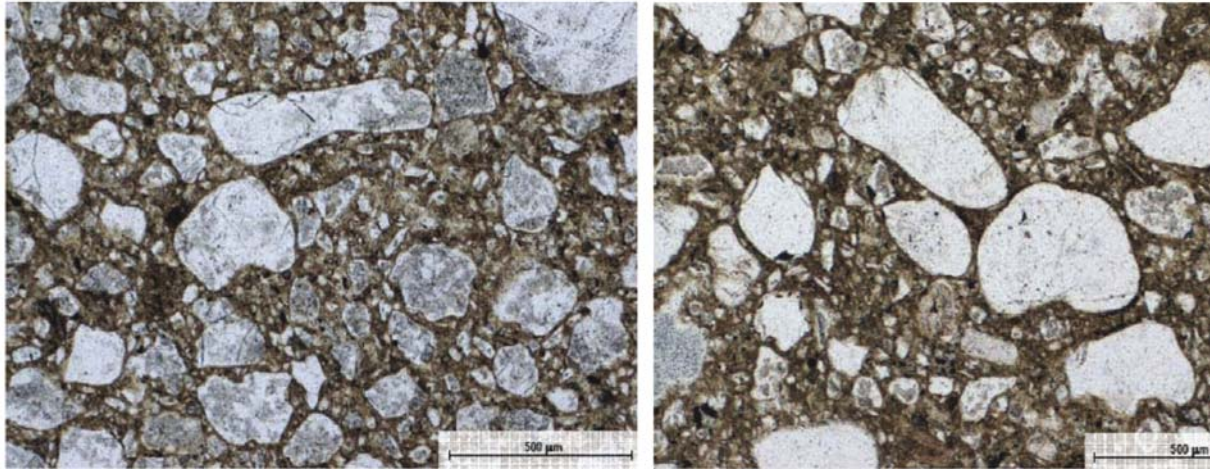
The tills of the Wartanian glaciation are more sandy, degraded in the upper part due to subsequent weathering processes. As a result of iron oxidation these soils are usually gray-brown. They are characterized by horizontal discontinuity surfaces. Their structure is illustrated by microscope images (Text-figs 3, 4) of samples in the natural state. This structure appears to be uniform

and stable as demonstrated by the lack of visible changes in the grain size distribution and cracks. Even the glauconite, the mineral with a small weathering resistance (green in the pictures), is not destroyed.

The tills of the Odranian glaciation, observed in all profiles are more compact and have a distinctive gray and dark gray colour. In the upper part of the profile their colour turns to brownish-gray. In the excavations, the vertical discontinuity surfaces are observed (joint).

The key to the proper assessment of the behaviour of cohesive soils of glacial origin is their reference to the geological position expressed by lithogenesis and to some extent by lithostratigraphy.

An important role in determining the origin of glacial clays (tills) plays the study of glacial sedimentation processes and their effects in present glaciated areas (i.a. Boulton 1972, Shaw 1977; Lawson 1979). These studies allow us to distinguish the basic genetic types of the tills, considering the deposition process as a criterion (Boulton 1976). Over the past thirty years, intensive research on the genesis of the Pleistocene tills has been carried out (i.a. Rusczyńska-Szenajch 1983 1998; Brodzikowski and Van Loon 1991; Hart and Boulton 1991; Piotrowski *et al.* 1997; Hart 1998). On the basis of the research and observation of processes occurring today in the glacial environment, three genetic types of tills were distinguished (Dreimanis 1989; Boulton 1976):



Text-fig. 3. The structure of undisturbed tills from Nowoursynowska Street (Nu). Samples taken from 6 m below the surface. Polarizing microscope;  $\times 50$

- lodgement till – this sediments is formed directly under moving ice by deposition of the substrate material located in the lower part of the glacier,

- melt-out till – this sediments arises from melting of dead ice cementing the moraine material,

- flow till – this sediments is created when melted material is so hydrated that IT is moved by gravity.

The field tests (Trzciński 1998b) allowed the identification of the characteristics of the tills from the exposures at the Nowoursynowska Street site **Nu** (Text-fig. 5), and the Kiedacza Street site **Kd** (Text-fig. 6). The tills were classified as the “lodgement tills” type.

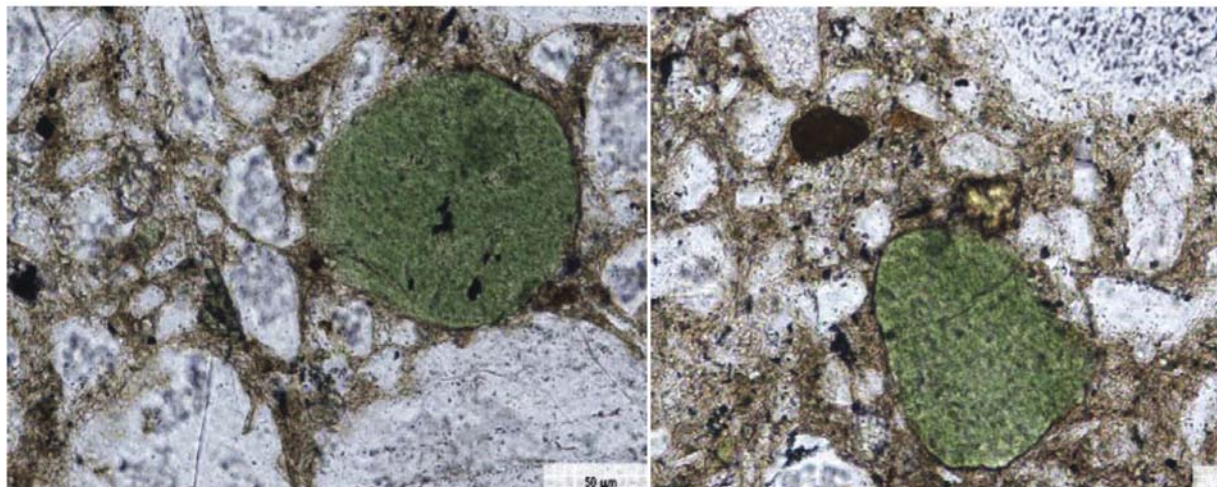
comprehensive study, as well as the determination of the impact of various external factors on the variability of the tested parameters. In this article selected elements of a broad research program (Kaczyński *et al.* 2008a) were analyzed and reinterpreted including both observations and field studies as well as advanced laboratory tests. The aim of linking together the test results obtained was the assessment of selected soil behaviours under specified loads and comparable verification of used test methods (Text-fig. 7).

#### Field tests

The preliminary geological work and drilling allowed for the identification of soil and water conditions, profile description and the collection of high-quality samples for laboratory tests. All essential laboratory tests were carried out on undisturbed sam-

#### METHODOLOGY

Determination of the representative characteristics of engineering-geological conditions requires a



Text-fig. 4. The structure of undisturbed tills from Nowoursynowska Street (Nu). Samples taken from 6 m below the surface. Polarizing microscope;  $\times 200$

ples obtained by means of thin-wall open tube samplers of the Shelby type.

Based on field tests CPT(u) and DMT the set of stress history parameters was obtained. The permeability parameters were collected by means of the groundwater monitoring system BAT.

The static probe (CPT) is one of the most widely used in-situ test methods of determining soil properties (Lunne *et al.* 1997; Młynarek and Wierzbicki 2007; Sikora 2006). Standardized cone resistance  $q_c$  and sleeve friction  $f_s$  are registered during the test. The GOUDA device and hardware were used in the test, according to the requirements of an appropriate standard.

The dilatometer test (DMT) allows the assessment of a number of soil parameters, but it is particularly useful in a reliable assessment of compressibility modulus and the horizontal component of the stress existing in the soil (Marchetti 1980). The DMT consists of a stainless steel blade with a thin flat circular expandable steel membrane on one side. When at rest, the external surface of the membrane is flush with the surrounding flat surface of the blade. The blade is connected to a control unit on the surface by a nylon tube containing an electrical wire and is pushed into the ground using the CPT rig. At 0.2 m depth intervals pushing is stopped and the membrane is inflated by means of pressurized gas. Readings are taken of the A-pressure required to begin to move the membrane and of the B-pressure required to move its centre 1 mm horizontally into the soil. During the tests, in addition to the above, it is also possible to determine the undrained shear stress, the overconsolidation ratio and to predict the soil type in the geological profile.

The piezometer of the BAT type was firstly used by Torstensson (1984). The BAT system may be used for testing poorly permeable soil with permeability coefficient  $k < 10^{-6}$  m/s. The measurement methodology has

been described in numerous studies, i.a.: Torstensson and Petsonk (1986), Petsonk *et al.* (1989), Krogulec (1992, 1997), and Sobolewski and Bajda (2001). The BAT probe, protected by a guide pipe, is statically pressed into the soil along with the filter. The filter tip is equipped with a rubber seal. During the test the seal is penetrated by a double ended injection needle. Conducting a test is possible after interconnection of filter tip placed in the soil, test container and pressure transducer.

The “out flow”-type tests were conducted. Before the test, there was an overpressure generated in the test container so that during a test the water flows from the test container interconnected with the filter tip to the surrounding layers of the peat. The basis of the methodology of the hydraulic conductivity in the BAT method are the gas laws (Boyle-Mariotte’s, Gay-Lussac’s and Clapeyron’s) and registration of the change of pressure inside the test container. The observation of the rate of these changes, directly related to the amount of the flowing water and thus the permeability of the soil, allows the calculation of the hydraulic conductivity. Before each measurement, the value of the pore water pressure was determined, which was required to calculate the horizontal hydraulic conductivity from the equation of Torstensson and Petsonk (1986).

### Microstructure research

The qualitative and quantitative analyses of the microstructures using the scanning electron microscope (SEM) is used widely in many fields of geology, particularly in engineering-geology (Osipov *et al.* 1984, 1989; Sokolov 1990; Kaczyński and Trzeciński 1997; Trzeciński 1998a, 2004; Gratchev *et al.* 2006). The test specimens for microstructure research were taken at 24 depths from 3 profiles (boreholes). The



Text-fig. 5. Grey-brown tills from Nowoursynowska Street (Nu). Clearly visible discontinuity surfaces



Text-fig. 6. Tills from Kiedacza Street (Kd). Horizontal and angular discontinuity surfaces and protruding cobbles are visible in the middle

following depths were sampled: from 4.6 to 23.2 m in **Ct**, from 2.9 to 11.2 m in **Kd** and from 2.7 to 9.3 m in **Nu**. In order to determine the effect of the load on microstructural changes, especially in the pore space, the samples from **Nu** borehole were selected at depths from 9.0 to 9.35 m below the surface. Two undisturbed samples were analyzed before the load application and the corresponding two after load application. One of them was loaded with a slow and the second with a rapid load increment, both up to a maximum value of 20 MPa. The quantitative analyses of the microstructure of the tills was conducted in a scanning electron microscope (SEM) Jeol, type JSM-6380LA using secondary electron emission (SE). The images of high resolution were recorded with a magnification range from 50 to 12 800 times. Preparation of test specimens required the actual behaviour of the structural system of the soil with particular accent on the surface of the prepared samples. Low temperature drying was applied by the sublimation in vacuum method (Tovey and Wong 1973; Smart and Tovey 1982; Kaczyński and Trzciniński 1997; Shi *et al.* 1999; Trzciniński 2004). As revealed by experiments (Osipov 1979), drying by means of this method produces the smallest changes in linear and volumetric structure of cohesive soils. For all collected samples, the analysis of the vertically oriented surface was conducted. For quantitative analysis of till microstructure, the STIMAN software was used (Sergeev *et al.* 1984, 1985; Sokolov *et al.* 2002). The set of parameters was determined including morphometric parameters: diameter  $D$ , area  $S$ , pore perimeter  $P$ , porosity  $n$  and the total number of pores  $N$ ) and geometric parameters: shape of the pores based on the form index of pores  $K_f$ , orientation of the structural elements on the orientation diagram (rose) and microstructure anisotropy index  $K_a$ .

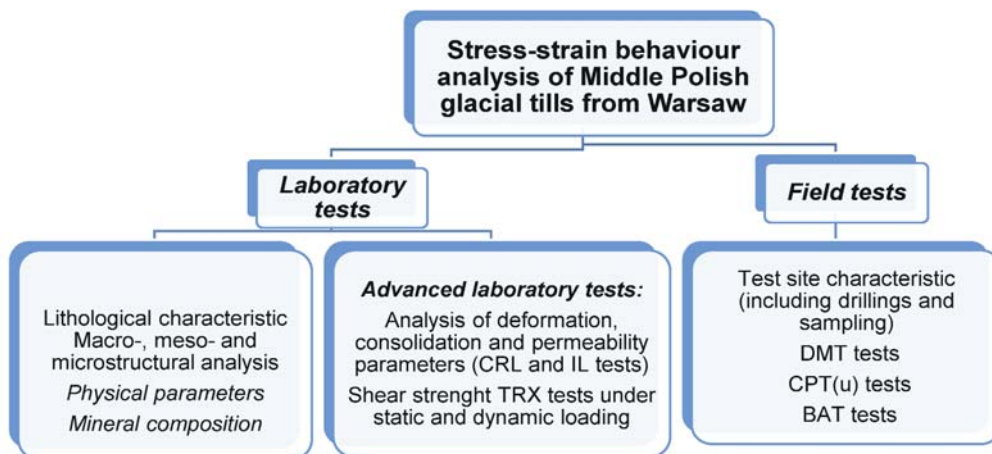
**Physical and mechanical propertie**

The field and laboratory tests of the physical properties and the strength and deformation parameters of tills was carried out according to the recommendations given in the standards (PN-88 / B-04481, ASTM), and textbooks (Head 1992, 1994; Grabowska-Olszewska 1998; Myślińska 2006). The terms and symbols were adopted from PN-B-02481 standard.

The study of the mineral composition was conducted in Labsys™ TG-DTA12 apparatus manufactured by Setaram. The following conditions were used: weight to 40 to 80 mg, sensitivity adjusted automatically by the apparatus, heating speed 10°C/min and helium atmosphere. In order to determine the quantitative mineral composition, for each sample derivatograms of the fraction less than 2 mm were obtained. The fraction was separated by means of the sedimentation method. Identification and quantitative determination of the proportion of clay minerals was based on the knowledge of dehydration (dh), dehydroxylation (dho), the range of temperatures at which they were observed and the presence or absence of a kaolinite peak (Kościółko and Wyrwicki 1996).

**Soil suction tests**

Extension of the physical characteristic of soils includes soil volume changes correlated with the degree of saturation. The parameter used to estimate the potential field heave is soil suction, which most accurately describes the unsaturated/partially saturated soil state. Soil suction is a macroscopic property that indicates the intensity or energy level with which a soil sample attracts water and incorporates overall properties (e.g., physical, chemical and mineralogical properties). Soil



Tekst-fig. 7. Range of advanced geological engineering studies of Middle Polish glaciation tills

suction tests were conducted on undisturbed and disturbed samples using the filter paper method according to ASTM D 5298-94 by Whatman paper No. 42. The relationship between water content and soil suction, so-called soil-water characteristic curves (SWCC) for Odranian and Wartanian tills was determined. Tests were carried out from 1 kPa to 1580 kPa (4.2 pF) using manual pressure plates model 1500 produced by Moisture Equipment Corporation.

### Deformation properties

Deformation tests were focused on determining the geological load history. The tests were carried out using both the original author’s design of consolidometer construction capable to achieve high loads up to 20 MPa (Text-fig. 8) and standard Rowe-Barden consolidometer with a range of stress up to 2 MPa.

In the high-pressure consolidometer a total number of 25 load steps (IL system) with various increments of stress adjusted to the increasing stiffness of the soil was conducted (Table 1). The duration of each load level was 24 hours, which practically enabled the end of the filtration stage of the consolidation process and was consistent with the transitional procedures for CL tests methodology. In high-pressure studies due to safety requirements and the efficiency of the construction solutions a hybrid technique of pneumatic-hydraulic loading was chosen. An essential element of this 3-step system is an air-oil pump of maximator type with a 1:200 gear ratio. The device is supplied with compressed air from the compressor piston. Maximator forced the pressure in the hydraulic oil which was served to the corresponding pressure accumulator. Its role was to maintain the constant load value despite the settlement of a soil sample.

Consolidometer tests performed under a constant rate of loading (CRL) were carried out in Rowe-Barden chamber. A constant rate of loading as well as de-

formation and pore pressure record was possible due to the computer-control system of two controllers: pressure and water volume. The system was manufactured by the British company GDS Instrument Ltd. These devices allowed the application on the sample of an external stress up to the value of 2000 kPa with an accuracy of 1 kPa. The software calculates the deformation of the sample on the basis of the measurement of the volume of liquid flowing out from the controller (accuracy 1 mm<sup>3</sup>). This optionally may also be measured by an external, analogue or digital sensor. The second driver is used for measurements of pore pressure during the test or for measurements of the volume of water flowing out of the soil.

### Dynamic shear strength tests

The study were conducted on undisturbed samples prepared according to the procedure of back pressure saturation and isotropic consolidation ( $\sigma'c = 100$  kPa) prior to a loading step.

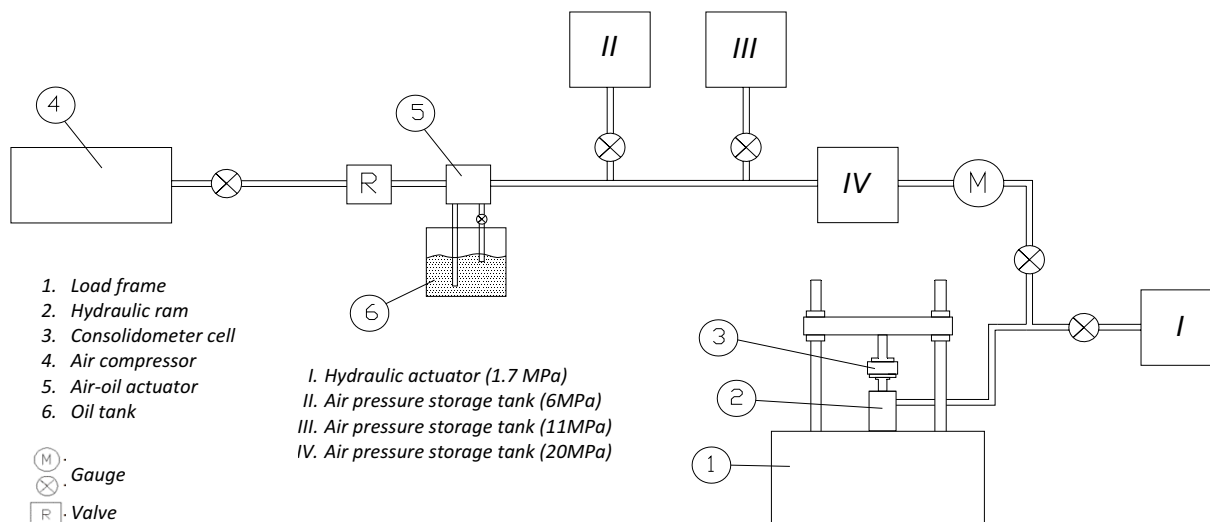
In order to determine the load conditions, field measurements of soil vibrations induced by road traffic were conducted. This way it was possible to establish the frequencies and ranges of vibration acceleration occurring in an urban area (Kaczyński *et al.* 2012). These measurements allowed the restoration of load conditions with a similar intensity to actual ones.

The evaluation of the effect of dynamic loading on the soil strength was determined using an alternative procedure: post-cyclic research carried out under static load, applied immediately after the phase of dynamic loading under axial displacement control conditions and a test under constant stress amplitude (load control conditions) (Text-fig. 9).

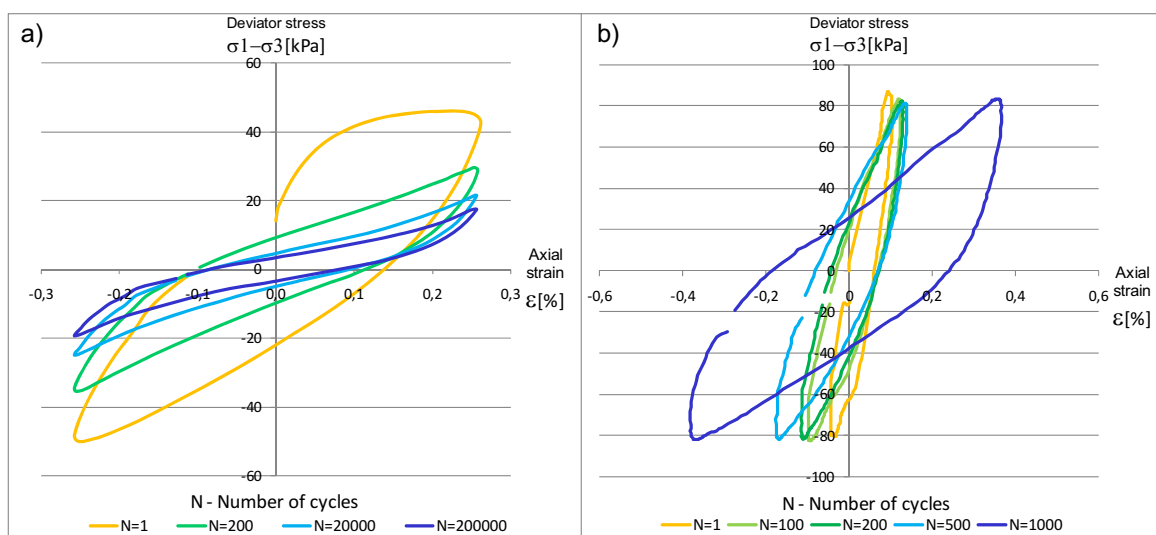
Dynamic loading of samples under undrained conditions were carried out at a frequency of 10 Hz with a constant amplitude of axial displacement of 0.1 and 0.4 mm. This was a guarantee of the constant vibration

| Load steps | Range of stress [MPa] | Stress increment [MPa] | Loading system components<br>(max pressure values showed in brackets)  |                                    |
|------------|-----------------------|------------------------|--|------------------------------------|
| 1 – 14     | 0.05–0.7              | 0.05                   | hydraulic subsystem :<br>- hydraulic ram<br>- hydraulic actuator (1.7 MPa)   |                                    |
| 15         | 0.7–1.0               | 0.3                    |  |                                    |
| 16         | 1.0–1.2               | 0.2                    |  |                                    |
| 17         | 1.2–1.5               | 0.3                    | pneumatic-hydraulic subsystem:<br>- air compressor (1.1 MPa)<br>- air-oil actuator with pressure increase ratio 1:200 (maximator M 189L. with regulator and gauge) | Air pressure storage tank (6 MPa)  |
| 18         | 1.5–3.0               | 0.5                    |  | Air pressure storage tank (11 MPa) |
| 19 – 20    | 3.0–5.0               | 1.0                    |  |                                    |
| 21 – 23    | 5.0–9.0               | 2.0                    |  |                                    |
| 24         | 9.0–15.0              | 6.0                    |  |                                    |
| 25         | 15.0–20.0             | 5.0                    | Air pressure storage tank (20 MPa)   |                                    |

Table 1. Number and range of stress stages used in high pressure consolidometer tests



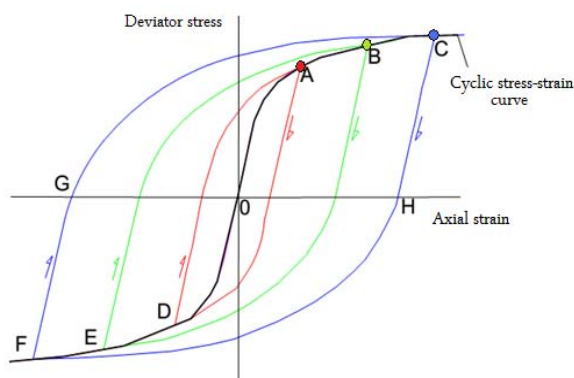
Text-fig. 8. Scheme of high pressure consolidometer



Text-fig. 9. Examples of hysteresis loops of selected load cycles with constant amplitude of (a) axial displacement (b) stress

acceleration maintenance. 200 000 cycles of two way cyclic loading with a sine input wave were applied. After a dynamic stage, the samples were submitted to post-cyclic compression in static conditions. Static tests were performed under undrained conditions (CU type test) with constant value of axial displacement of 0.012 mm/min (approx. 1% of axial strain/h). Based on the difference between the value of deviator stress at failure in post-cyclic tests and the corresponding value of deviator stress obtained from static tests, the percentage loss of soil strength was determined.

In studies with a constant stress amplitude, the limit stress value which would affect the soil strength was required. After determining the maximum value of de-



Text-fig. 10. Cyclic stress-strain curve defined as a vertex of stabilized hysteresis loop



viator stress under static loading the limit stress amplitude values were determined under dynamic loading. These values were determined as the cyclic stress ratio CSR, which was defined by the ratio of the amplitude of the tangential shear stress to the soil shear strength determined during monotonic shear (Green and Terri 2005). The tests were carried out for CSR coefficients ranging from 0.2 to 0.6 and each phase consisted of A loading and unloading phase at 10 000 cycles.

In order to determine the stress-strain relation in dynamic loading the soil samples were tested under a constant initial conditions and different amplitudes of load. This procedure allowed us to determine cyclic stress-strain curve (Text-fig. 10).

TEST RESULTS AND DISCUSSION

Physical parameters

The tested soils are of Pleistocene age (Middle Polish Glaciation period), developed mainly as sandy clays (tills) with average contents of: clay 14.3–17.5%, silt 22.3–24.0% and sand 56.5–61.1% (Table 2). The glacial tills classified to the Odranian glaciation period are “less sandy” than tills classified to the Wartanian glaciation. The natural bulk density ranges from 2.09–2.29 Mg/m<sup>3</sup>, whereas the bulk density of Odranian tills was characterized by higher values than Wartanian tills. The total

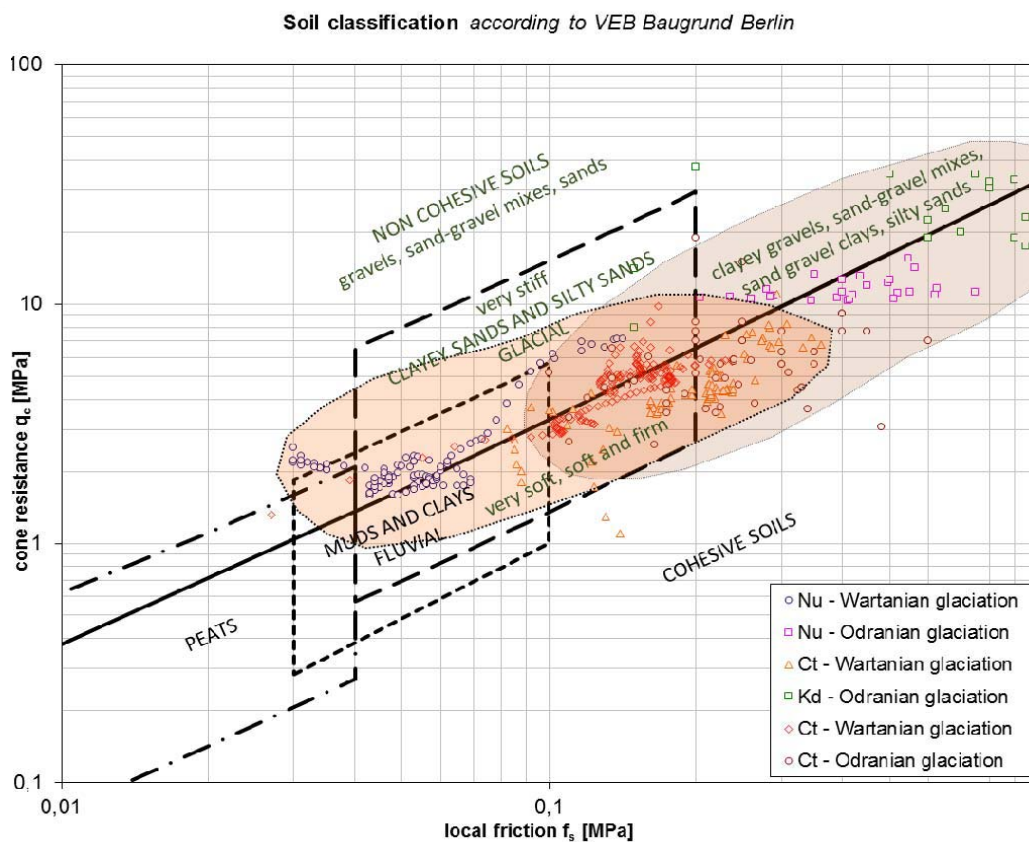
porosity n of tested tills was on average 26%. The natural consistency of tested tills was stiff and firm. The liquidity index I<sub>L</sub> varied from 0.29 to 0.21. The plasticity index I<sub>p</sub> was approx. 13%. The consistency index I<sub>c</sub> = 1 – I<sub>L</sub> for all tested samples was on average 1.02 indicating consolidation of these soils. Variation coefficients V of particular parameters indicate the specific character of each parameter and the methodology of their determination (Dobak 1984; Lee *et al.* 1983). The highest V values were recorded for liquidity index I<sub>L</sub> and plasticity index I<sub>p</sub>. Their specific deposition character was reflected in the variability of physical parameters in general but especially in the variability of silt and clay content. Odranian tills from Ct site are different from those obtained from other sites. These firm soils occurred deeper in the profile and had a higher water content, porosity and liquidity index but a lower sandy fraction content. Despite this, on the basis of a comparison of the properties of tills occurring in Ursynów district with the characteristics for these tills from the Warsaw area (Frankowski and Wysokiński 2000) it can be concluded that the tested tills were more consolidated (with a lower water content, lower liquidity index and higher bulk density). In terms of particle size distribution, Służew (Ct) tills are more clayey and the average content of clay of Warsaw tills was lower than of those from Ursynów.

The results of CPT tests may be a comparative reference to the soil topology based on laboratory tests. CPT results plotted on chosen classification charts

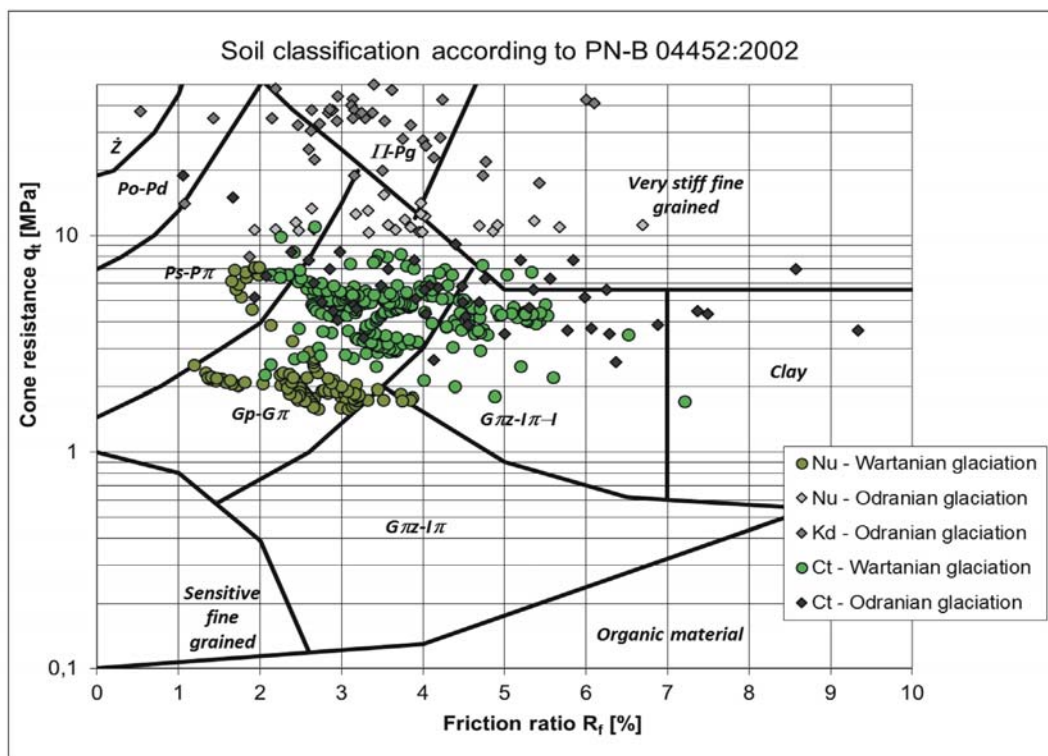
| Glaciations | Parameter | Solid density ρ <sub>s</sub> [Mg/m <sup>3</sup> ] | Wet/bulk density ρ [Mg/m <sup>3</sup> ] | Dry density ρ <sub>d</sub> [Mg/m <sup>3</sup> ] | Porosity n [%] | Void ratio e [-] | Degree of saturation S <sub>r</sub> [-] | Water content w <sub>n</sub> (%) | Plastic limit w <sub>p</sub> (%) | Liquid limit w <sub>L</sub> (%) | Plasticity index I <sub>p</sub> (%) | Liquidity index I <sub>L</sub> (-) | Grain size distribution |          |               |          |
|-------------|-----------|---|---|---|----------------|------------------|---|----------------------------------|----------------------------------|---------------------------------|-------------------------------------|------------------------------------|-------------------------|----------|---------------|----------|
|             |           |   |   |   |                |                  |   |                                  |                                  |                                 |                                     |                                    | > 2 mm                  | 2–0,05mm | 0,05–0,002 mm | 0,002m m |
| WARTANIAN   | $\bar{x}$ | 2.67  | 2.19                                    | 1.96  | 0.36           | 0.26             | 0.86                                    | 11.5                             | 12.8                             | 25.5                            | 12.7                                | -0.01                              | 2.4                     | 61.1     | 22.3          | 14.3     |
|             | σ         | 0.01  | 0.04                                    | 0.05  | 0.04           | 0.02             | 0.09                                    | 1.87                             | 0.90                             | 6.89                            | 6.12                                | 0.17                               | 3.38                    | 14.15    | 10.77         | 5.37     |
|             | min       | 2.66  | 2.11                                    | 1.85  | 0.33           | 0.25             | 0.73                                    | 9.1                              | 12.2                             | 19.1                            | 6.7                                 | -0.29                              | 0.0                     | 30.0     | 14.0          | 10.0     |
|             | max       | 2.69  | 2.25                                    | 2.01  | 0.45           | 0.31             | 1.06                                    | 14.3                             | 14.3                             | 36.8                            | 22.5                                | 0.17                               | 10.0                    | 70.0     | 47.0          | 23.0     |
|             | v         | 0.00  | 0.02                                    | 0.03  | 0.11           | 0.08             | 0.11                                    | 0.16                             | 0.07                             | 0.27                            | 0.48                                | >1                                 | >1                      | 0.23     | 0.48          | 0.38     |
|             | n         | 7   | 9                                       | 9   | 9              | 9                | 9                                       | 13                               | 5                                | 5                               | 5                                   | 5                                  | 8                       | 8        | 8             | 8        |
| ODRANIAN    | $\bar{x}$ | 2.67  | 2.20                                    | 1.97  | 0.36           | 0.26             | 0.89                                    | 11.8                             | 12.0                             | 25.0                            | 13.0                                | -0.03                              | 2.0                     | 56.5     | 23.9          | 17.5     |
|             | σ         | 0.02  | 0.05                                    | 0.07  | 0.05           | 0.03             | 0.09                                    | 2.27                             | 1.41                             | 7.05                            | 5.82                                | 0.12                               | 1.46                    | 12.57    | 9.60          | 5.25     |
|             | min       | 2.66  | 2.09                                    | 1.85  | 0.30           | 0.23             | 0.68                                    | 9.1                              | 10.7                             | 18.9                            | 6.7                                 | -0.27                              | 0.0                     | 32.0     | 8.0           | 5.0      |
|             | max       | 2.75  | 2.29                                    | 2.10  | 0.45           | 0.31             | 1.08                                    | 16.6                             | 17.3                             | 48.1                            | 30.8                                | 0.21                               | 4.0                     | 83.0     | 48.0          | 28.0     |
|             | v         | 0.01  | 0.02                                    | 0.03  | 0.13           | 0.10             | 0.10                                    | 0.19                             | 0.12                             | 0.28                            | 0.45                                | >1                                 | 0.73                    | 0.22     | 0.40          | 0.30     |
|             | n         | 13  | 26                                      | 26  | 26             | 26               | 26                                      | 35                               | 20                               | 20                              | 20                                  | 19                                 | 15                      | 15       | 15            | 15       |

$\bar{x}$  - arithmetical mean; σ - standard deviation; min. max – minimum and maximum values; v – coefficient of variation; n – number of tests

Table 2. The variability of basic physical properties of tills from the region of Warszawa–Służew



Text-fig. 11. Soil classification according to VEB Baugrund Berlin for Nu, Ct and Kd profiles examined by CPT(u) tests



Text-fig. 12. Results of CPT(u) tests on the background of Robertson classification chart (PN-B-04452:2002)

give the evaluation of the soil type. According to the Berlin classification chart, the results are located mainly in the field described as stiff and firm clays and clays sands (Text-fig. 11) whereas the results obtained for Odranian tills are moved to the field representing the soils with less cohesion. In fact, the reason for such positioning was not low cohesion, but high strength and low water content. The same situation appears after plotting the results on a Robertson classification chart, according to which the majority of results refers to sandy or silty clays (Text-fig. 12) whereas the results obtained for Odranian tills are moved again to the field representing the soils with less cohesion. Such results mean that foreign classification charts have limited versatility and national or local correlations should be developed based on field and laboratory test results.

### Soil suction

The results of soil suction tests conducted by the filter paper method on Odranian and Wartanian till samples from **Ct**, **Nu** and **Kd** boreholes show differentiation. The average value obtained for Odranian tills is over 300 kPa, while for Wartanian tills is about 130 kPa (Kaczynski *et al.* 2008a). This variation may be related to differences in the lithology and mineral composition of the tills, especially in the subsurface area where moisture ratios (water content and degree of saturation) vary depending on the climatic conditions and on depth.

On the basis of the relationship between water content and soil suction (SWCC) the parameters proposed by McKeen (1992) to evaluate the soil expansiveness were determined for four selected samples of Odranian and Wartanian tills. These were: suction-water content index  $\Delta h/\Delta w$  (defined as the slope between the suction levels of 6–3 pF and water content changes  $\Delta w$ ) suction and compression index  $C_h$  (defined as the slope of the volume change-relation suction in the suction range of 2–2.5 pF to 5.5 pF) which represents soil response to the suction change. The results are presented in Table 3 and they show that the studied tills, under the mentioned classification, are in Class V – non-expansive soils, so they do not require special consideration for shrink and swell behavior. The calculations of the potential field heave of glacial tills from Warsaw based on suction measurements are presented in Izdebska-Mucha and Wójcik (2015).

### Mineral composition

The mineral composition of the clay fraction, determined by derivatography, is an important factor in-

fluencing the behaviour of cohesive soils. Analysis of the results obtained indicates that Wartanian tills at shallow depths and Odranian tills down to 13 m are characterized by a predominance of beidellite, whereas Odranian tills occurring at depths greater than 15 m have more illite minerals (Table 4). Greater amounts of beidellite in shallow parts of the profile can be caused by several factors, eg. weathering and diversity of ph in the environment.

The content of clay minerals varies with depth: in the shallow part of the profile it was about 11%, whereas in the deeper parts it was much higher – approx. 27%. Differences in the carbonate content were observed between Odranian and Wartanian tills as well. Calcite was predominant in Odranian tills whereas dolomite predominance was noticed in Wartanian tills. In the studied profiles, a significant dominance of goethite over siderite was also observed not only in Odranian tills occurring at depths greater than 15 m but also in Wartanian tills. On the other hand, in the shallower zones in Odranian tills the composition of these minerals was balanced as almost equal proportions – goethite 1% siderite 0.7%.

### Microstructure research

In the glacial tills studied, domination of matrix microstructure (occasionally matrix-skeletal microstructure) was observed (Sergeev *et al.* 1978, 1980; Grabowska-Olszewska *et al.* 1984).

The matrix microstructure (Text-fig. 13) was constructed mainly from the clay mass (matrix), where single grains of sand and silt are chaotically arranged. The Clay matrix was highly aggregated, creating micro-aggregates and aggregates. Micro-aggregates contact each other according to F-F, E-F and E-E types and no orientation of the structural elements exists. Pore space consists predominantly of isometric inter-micro-aggregate pores.

The matrix-skeletal microstructure (Text-fig. 14) means that the matrix microstructure was dominant, whereas a skeletal one occurs as local areas in the structure. The microstructure consists of more silty less sandy particles, that form a skeleton. Between the particles and on their surface there was chaotically arranged clay material. Clay particles condensed on the grain surface form clay halos. Clay material was distributed chaotically between the grains, forming a contact of a bridge type. Pore space was formed as evenly distributed, isometric inter-aggregate and inter-grain pores. No orientation of the structural elements was observed.

Compaction of structural elements in the tested

| Glaciation | Soil classification USCS (acc. ASTM D 2487-06) | Clay content CI [%] | Liquid limit LL [%] | Plasticity index PI [%] | Suction-water content index $\Delta h / \Delta w$ | Suction compression index $C_h$ [-] | Soil expansivity McKeen (1992) |
|------------|--|---------------------|---------------------|-------------------------|---|-------------------------------------|--------------------------------|
| W 1        | SC clayey sand                                 | 12                  | 23.0                | 10.5                    | -30.65  | -0.0133                             | nonexpansive                   |
| W 2        | SC-SM silty clayey sand                        | 10                  | 19.1                | 6.7                     | -25.79  | -0.0190                             | nonexpansive                   |
| O 1        | SC clayey sand                                 | 20                  | 22.3                | 11.2                    | -25.36  | -0.0251                             | nonexpansive                   |
| O 2        | SC clayey sand                                 | 15                  | 24.4                | 13.0                    | -30.68  | -0.0107                             | nonexpansive                   |

W – Wartanian glaciation deposits.  
 O – Odranian glaciations deposits

Table 3. Suction compression index ( $C_h$ ) and suction-water content index ( $\Delta h/\Delta w$ ) of glacial tills with McKeen (1992) classification of expansive soils

| Glaciation           | Statistical parameter | Percentage of individual components |            |        |           |         |          |         |          |                  |
|----------------------|-----------------------|-------------------------------------|------------|--------|-----------|---------|----------|---------|----------|------------------|
|                      |                       | Clay Minerals                       | Including: |        |           | calcite | dolomite | goethit | siderite | quartz and other |
|                      |                       |                                     | beidellite | illite | kaolinite |         |          |         |          |                  |
| Wartanian            | $\bar{x}$             | 11.6                                | 6.6        | 3.5    | 1.6       | 2.2     | 3.2      | 1.3     | 0.3      | 83.6             |
|                      | $\sigma$              | 6.7                                 | 4.3        | 2.6    | 1.2       | 1.7     | 3.2      | 0.7     | 0.3      | 8.2              |
|                      | min                   | 4.4                                 | 0.4        | 0      | 0.1       | 0       | 0        | 0.4     | 0        | 68.5             |
|                      | max                   | 23.2                                | 12.5       | 7.9    | 3.5       | 4.8     | 6.6      | 2.2     | 0.8      | 91.7             |
|                      | v                     | 0.58                                | 0.64       | 0.75   | 0.78      | 0.81    | 1.00     | 0.54    | 1.20     | 0.10             |
|                      | n                     | 8                                   | 8          | 8      | 8         | 8       | 8        | 8       | 8        | 8                |
| Odranian 0-13 m ppt  | $\bar{x}$             | 11.0                                | 7.8        | 3.3    | 1.6       | 4.6     | 0.7      | 1.0     | 0.7      | 82.0             |
|                      | $\sigma$              | 5.2                                 | 5.1        | 2.1    | 0.9       | 1.4     | 0.6      | 0.6     | 0.4      | 4.3              |
|                      | min                   | 4.1                                 | 2.4        | 0.1    | 0.4       | 1.2     | 0        | 0       | 0        | 74.5             |
|                      | max                   | 23.3                                | 20.3       | 5.3    | 3         | 6.8     | 1.7      | 2       | 1.3      | 87.5             |
|                      | v                     | 0.47                                | 0.65       | 0.64   | 0.58      | 0.30    | 0.88     | 0.59    | 0.56     | 0.05             |
|                      | n                     | 12                                  | 12         | 12     | 12        | 12      | 12       | 12      | 12       | 12               |
| Odranian 15-25 m ppt | $\bar{x}$             | 27.8                                | 8.9        | 14.0   | 4.9       | 4.6     | 2.6      | 1.6     | 0.1      | 64.9             |
|                      | $\sigma$              | 8.6                                 | 4.0        | 3.5    | 2.3       | 0.5     | 1.3      | 0.5     | 0.1      | 12.0             |
|                      | min                   | 16.3                                | 4.8        | 9.2    | 2.1       | 3.7     | 0.8      | 1       | 0        | 50.9             |
|                      | max                   | 38.2                                | 15.6       | 18.6   | 7.7       | 5       | 4.1      | 2.3     | 0.3      | 83.3             |
|                      | v                     | 0.31                                | 0.45       | 0.25   | 0.47      | 0.10    | 0.49     | 0.35    | 2.00     | 0.18             |
|                      | n                     | 5                                   | 5          | 5      | 5         | 5       | 5        | 5       | 5        | 5                |

Table 4. Mineral composition of tills

clays was observed. Tills taken from **Ct** site were characterised by changing degree of compaction from medium to dense. Tills taken from **Kd** site from the zone down to 5 m below the surface were characterised by a changing degree of compaction, loose to dense. No regularity was noted in structural compaction taking the age of the tills into consideration.

The presented qualitative assessment of the microstructure of glacial tills was confirmed by the parameters of the pore space determined on undisturbed till samples.

The general trends of the microstructure parameters could be formulated on the basis of the qualitative assessment of the Wartanian and Odranian tills (Table 5). Higher values of the porosity were observed in the sur-

face zone. A correlation between the number of pores  $N$  and porosity  $n$  was noticeable. The higher porosity was connected with the greater area of pores. A correlation between the total perimeter of pores with  $n$  value was observed as well. The microstructure anisotropy index was characterised by very low values, ranging between 2.5 and 15.0%, and occasionally up to 20%. These higher values were observed for tills from the **Ct** site.

The comparison of the microstructure parameters of the Wartanian and Odranian glacial tills led to the following conclusions:

- Differences in porosity and the number of pores are very small and slightly higher values were obtained for Odranian tills,
- Higher values of parameter for Odranian tills

were observed in case of total and maximum pore area and total and maximum pore perimeter whereas lower values were observed for average area and perimeter,

- Pore diameters (minimum, average and maximum as well) for both types of tills were comparable,
- In Odra tills the largest number of micropores and smaller number of mesopores was observed than in Warta tills,
- The values of microstructure anisotropy index was recorded for Odranian tills.

The impact of the load used in the studies (up to 20 MPa) at various load rates was noticeable and was reflected in the results of microstructural porosity analysis (Table 6). The following observations were made:

- The degree of compaction of structural elements for a slow increase of the load changed from medium to dense whereas at a rapid increase of the load – the compaction remained medium. In both cases, a de-

crease in porosity of about 3 – 6% after the load application was observed. The decrease was greater if a longer and slower load increment was applied,

- A decrease in the number of pores, total and minimum perimeter as well as the number of micro-pores and anisometric pores was observed,
- An increase of total, maximum and medium area of pores, pore perimeter as well as the number of mesopores and isometric pores together with an average coefficient of pore form was observed,
- No significant changes were observed in the minimum area and perimeter of pores and microstructure anisotropy index.

Noticeable changes were therefore observed in the value of the porosity and the number of pores. The reduction of the number of anisometric pores and micropores may suggest that during the additional load some of the pores became completely closed. That would explain why a relative increase of isometric

| Stratigraphy  | Wartanian glacial tills <sup>1)</sup> |        |         |                    |                              | Odranian glacial tills <sup>2)</sup> |        |         |                    |                              |
|---|---------------------------------------|--------|---------|--------------------|------------------------------|--------------------------------------|--------|---------|--------------------|------------------------------|
|   | min.                                  | max.   | average | standard deviation | coefficient of variation (%) | min.                                 | max.   | average | standard deviation | coefficient of variation (%) |
| Porosity $n$ [%]  | 19.4                                  | 27.7   | 23.8    | 2.8                | 12                           | 20.0                                 | 33.6   | 24.5    | 4.4                | 18                           |
| Number of pores $N \times 10^3$                           | 655                                   | 1850   | 1160    | 528                | 46                           | 965                                  | 2450   | 1730    | 483                | 28                           |
| Total pores area $S_t \times 10^3$ [ $\mu\text{m}^2$ ]    | 1800                                  | 6890   | 3930    | 2070               | 53                           | 1880                                 | 11500  | 4870    | 2590               | 53                           |
| Minimum pores area $S_{min}$ [ $\mu\text{m}^2$ ]          | 0.017                                 | 0.02   | 0.018   | 0.0009             | 5                            | 0.017                                | 0.02   | 0.017   | 0.0005             | 3                            |
| Maximum pores area $S_{max}$ [ $\mu\text{m}^2$ ]          | 51100                                 | 120000 | 91000   | 29500              | 32                           | 24800                                | 290000 | 98500   | 69000              | 70                           |
| Average pores area $S_{av}$ [ $\mu\text{m}^2$ ]           | 1.31                                  | 10.52  | 4.48    | 3.8                | 85                           | 1.04                                 | 8.79   | 3.18    | 2.3                | 72                           |
| Total pores perimeter $P_t \times 10^3$ [ $\mu\text{m}$ ] | 3560                                  | 6590   | 5150    | 1080               | 21                           | 4140                                 | 11100  | 7370    | 2240               | 30                           |
| Minimum pores perimeter $P_{min}$ [ $\mu\text{m}$ ]       | 0.7                                   | 1.27   | 1.04    | 0.2                | 19                           | 0.66                                 | 1.41   | 0.9     | 0.25               | 0.28                         |
| Maximum pores perimeter $P_{max}$ [ $\mu\text{m}$ ]       | 8600                                  | 11900  | 10300   | 1410               | 14                           | 5040                                 | 33100  | 13500   | 8410               | 62                           |
| Average pores perimeter $P_{av}$ [ $\mu\text{m}$ ]        | 3.12                                  | 7.53   | 5       | 1.7                | 34                           | 2.66                                 | 7.48   | 4.45    | 1.5                | 34                           |
| Minimum pores diameter $D_{min}$ [ $\mu\text{m}$ ]        | 0.15                                  | 0.15   | 0.15    | -                  | -                            | 0.15                                 | 0.15   | 0.15    | -                  | -                            |
| Maximum pores diameter $D_{max}$ [ $\mu\text{m}$ ]        | 255                                   | 391    | 336     | 57                 | 17                           | 178                                  | 608    | 338     | 111                | 33                           |
| Average pores diameter $D_{av}$ [ $\mu\text{m}$ ]         | 0.36                                  | 0.79   | 0.56    | 0.2                | 36                           | 0.37                                 | 0.82   | 0.54    | 0.1                | 19                           |
| Micropores $0.1 < \emptyset < 10 \mu\text{m}$ [%]         | 7.6                                   | 33.6   | 18.4    | 10.3               | 56                           | 4.6                                  | 43     | 22.6    | 12.4               | 55                           |
| Mezopores $10 < \emptyset < 1000 \mu\text{m}$ [%]         | 66.4                                  | 92.4   | 81.6    | 10.3               | 13                           | 57                                   | 95.4   | 77.4    | 12.4               | 16                           |
| Minimum form index of pores $K_{fmin}$ [-]                | 0                                     | 0.028  | 0.005   | 0.011              | 220                          | 0                                    | 0.059  | 0.016   | 0.02               | 125                          |
| Maximum form index of pores $K_{fmax}$ [-]                | 0.946                                 | 0.99   | 0.958   | 0.017              | 2                            | 0.911                                | 0.991  | 0.958   | 0.02               | 2                            |
| Average form index of pores $K_{fav}$ [-]                 | 0.393                                 | 0.504  | 0.469   | 0.04               | 9                            | 0.377                                | 0.506  | 0.452   | 0.05               | 11                           |
| Izometric pores $a/b < 1.5$ [%]                           | 10.9                                  | 20     | 15.8    | 3.4                | 22                           | 6.5                                  | 22.1   | 15.9    | 4.9                | 31                           |
| Anisometric pores $1.5 < a/b < 10$ [%]                    | 80                                    | 89.1   | 83.9    | 3.2                | 4                            | 77.9                                 | 92.1   | 83.3    | 4.6                | 6                            |
| Fissure-like pores $a/b > 10$ [%]                         | 0                                     | 1.6    | 0.3     | 0.6                | 200                          | 0                                    | 3      | 0.8     | 0.9                | 113                          |
| Microstructure anisotropy index $K_a$ [%]                 | 1.2                                   | 28     | 7.8     | 10                 | 128                          | 2.4                                  | 21.1   | 9.4     | 5.8                | 62                           |

<sup>1)</sup> – number of samples 6. <sup>2)</sup> – number of samples 18.  $\emptyset$  – the equivalent diameter of pores.  $a/b$  – the ratio between two most different dimensions of pore.

Table 5. Comparison of the results of quantitative microstructural SEM analysis of Wartanian and Odranian tills (statistics)

| Sample name   | gr 3a-6 <sup>1)</sup> | gr 3a-6k <sup>2)</sup> | gr 3a-7 <sup>1)</sup> | gr 3a-7k <sup>3)</sup> |
|---|-----------------------|------------------------|-----------------------|------------------------|
| Porosity $n$ [%]  | 22.67                 | 16.40                  | 23.87                 | 19.99                  |
| Number of pores $N \times 10^3$                           | 1119                  | 943                    | 1987                  | 877                    |
| Total pores area $S_t \times 10^3$ [ $\mu\text{m}^2$ ]    | 2100                  | 2404                   | 2193                  | 1875                   |
| Minimum pores area $S_{min}$ [ $\mu\text{m}^2$ ]          | 0.017                 | 0.018                  | 0.017                 | 0.018                  |
| Maximum pores area $S_{max}$ [ $\mu\text{m}^2$ ]          | 75471                 | 99359                  | 70661                 | 85794                  |
| Average pores area $S_{av}$ [ $\mu\text{m}^2$ ]           | 1.88                  | 2.55                   | 1.10                  | 2.14                   |
| Total pores perimeter $P_t \times 10^3$ [ $\mu\text{m}$ ] | 4857                  | 4231                   | 6739                  | 3761                   |
| Minimum pores perimeter $P_{min}$ [ $\mu\text{m}$ ]       | 1.10                  | 0.84                   | 0.88                  | 0.92                   |
| Maximum pores perimeter $P_{max}$ [ $\mu\text{m}$ ]       | 9529                  | 17263                  | 7650                  | 11891                  |
| Average pores perimeter $P_{av}$ [ $\mu\text{m}$ ]        | 4.34                  | 4.49                   | 3.39                  | 4.29                   |
| Minimum pores diameter $D_{min}$ [ $\mu\text{m}$ ]        | 0.15                  | 0.15                   | 0.15                  | 0.15                   |
| Maximum pores diameter $D_{max}$ [ $\mu\text{m}$ ]        | 310                   | 356                    | 300                   | 331                    |
| Average pores diameter $D_{av}$ [ $\mu\text{m}$ ]         | 0.50                  | 0.54                   | 0.38                  | 0.50                   |
| Micropores $0.1 < \varnothing < 10$ $\mu\text{m}$ [%]     | 25.9                  | 20.8                   | 25.4                  | 24.1                   |
| Mezopores $10 < \varnothing < 1000$ $\mu\text{m}$ [%]     | 74.1                  | 79.2                   | 74.6                  | 75.9                   |
| Minimum form index of pores $K_{fmin}$ [-]                | 0.044                 | 0.078                  | 0                     | 0                      |
| Maximum form index of pores $K_{fmax}$ [-]                | 0.983                 | 0.990                  | 0.952                 | 0.944                  |
| Average form index of pores $K_{fav}$ [-]                 | 0.492                 | 0.498                  | 0.467                 | 0.475                  |
| Izometric pores $a/b < 1.5$ [%]                           | 18.5                  | 24.8                   | 14.9                  | 15.8                   |
| Anisometric pores $1.5 < a/b < 10$ [%]                    | 81.5                  | 75.2                   | 84.3                  | 84.1                   |
| Fissure-like pores $a/b > 10$ [%]                         | 0                     | 0                      | 0.8                   | 0.1                    |
| Microstructure anisotropy index $K_a$ [%]                 | 1.9                   | 2.2                    | 6.2                   | 5.4                    |

<sup>1)</sup> – the sample of the natural structure before additional load.

<sup>2)</sup> – the sample after additional load of 20 MPa with a slow increase of load.

<sup>3)</sup> – the sample after additional load of 20 MPa with a rapid increase of load.

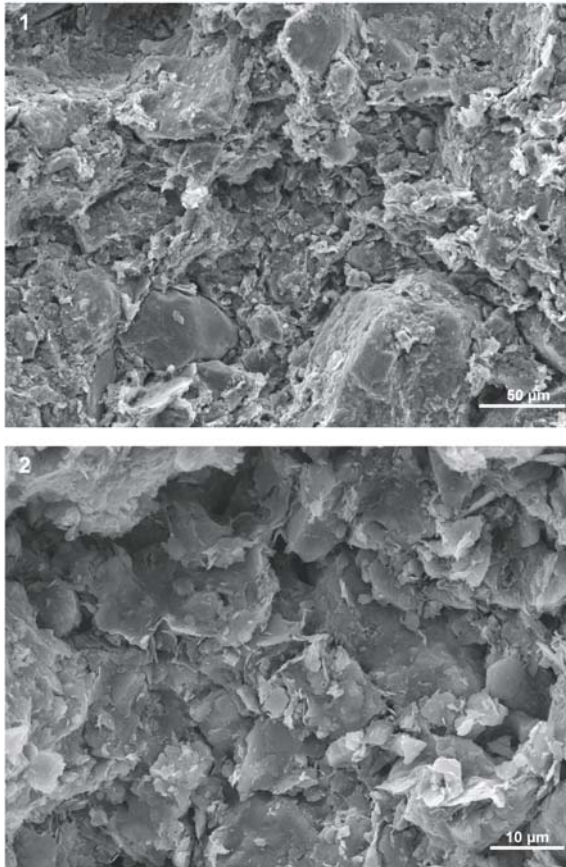
Table 6. Results of quantitative microstructural SEM analysis of tills (samples after one-dimension compressibility test)

pores and mesopores, total maximum and medium area of pores, maximum and medium pore perimeter and diameter was observed.

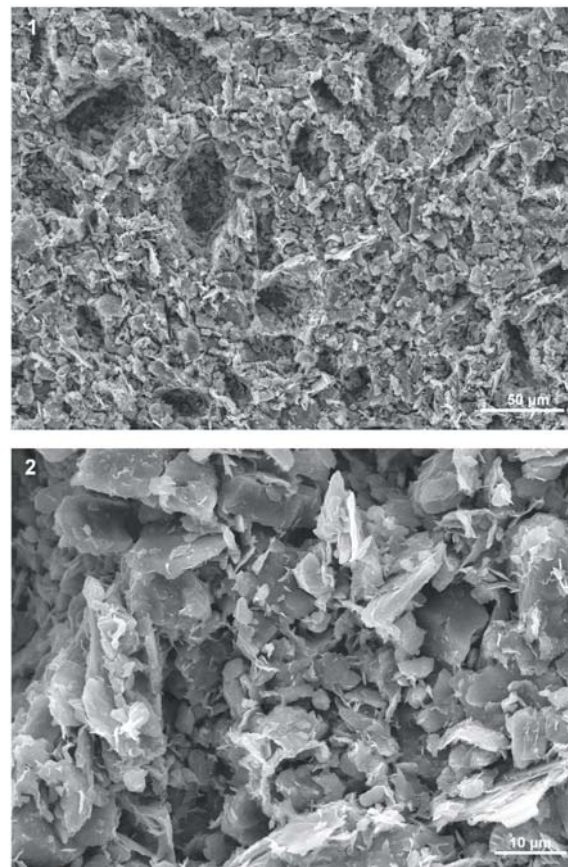
The applied load did not cause any significant changes in the anisotropy of the microstructure. A small range of microstructural changes caused by an additional load of till samples may indicate that the tested material had already been subjected to additional loads in geological history (eg. by the Warta glacier). In addition, the fact that this till was created with the participation of a lodgement process under the slight hydration conditions below the foot of an active glacier should also be considered. Depositional conditions suggest that tested till was a lodgement type till (Ruszczynska-Szenajch *et al.* 2003; Trzcinski 1998b). As a result of this mechanism of deposition, friction plays a crucial role in the release of the frozen moraine from a moving glacier. This type of release could cause high degree of compaction, and an additional break in sedimentation (seen as frequent discontinuity surfaces underlined by ferrous traces) caused additional compaction of the material during the glacier sliding over a formerly deposited till.

## Deformation parameters assessment

The field and laboratory tests program prepared for this research, allowed us to obtain the characteristics of soil compressibility. The comparison of the results from both methods was based on such stress state at which the test modules were obtained in the dilatometers test (DMT) and consolidometer tests (CRL). This significantly limited the comparative material, as DMT modules were obtained usually at larger stresses than it was for Rowe-Barden consolidometer. On the other hand, the limitation of the scope of the analyzed loads to lower values, brought better characteristics for shallow parts of the profile where more deformable soils occur. This was confirmed in this study (Text-fig. 15). The DMT modules within the range of 10 to 30 MPa were generally lower than the mean values of modules obtained in the CRL. The exponential approximation of the analyzed relation between the  $M_{DMT}$  and  $M_{CRL}$  intersected the dashed line of the equivalence of these modules at a value of 40 MPa. Furthermore, significantly higher values of the modules of the dilatometer in relation to the results of consolidometer tests were obtained. The impact of the aforementioned relation of modules and stresses at which



Text-fig. 13. Matrix microstructure of till from Nowoursynowska Nu (description in the text); SEM, 1 ×400, 2 ×1600



Text-fig. 14. Matrix-skeletal microstructure of till from St. Catherine Church (Ct) (description in the text); SEM, 1 ×400, 2 ×1600

those modules were determined clearly indicates a significant increase in DMT to more than 40 MPa in comparison to the laboratory results. Significant dispersion of the results indicates the necessity of a careful assessment of module variability in estimation of the derived values of deformability parameters.

As the basis of CPT(u) and DMT tests a number of mechanical parameters were determined *in situ*. The constrained modulus  $M$  is one of the important characteristics of soil. The value obtained from a DMT test is particularly important. The conditions of its determination in this test are similar to the fundamental criteria used in soil mechanics. During the DMT test the range of soil stresses is registered, for which a known deformation (1.1 mm) is assigned. Therefore, this parameter is treated as a benchmark for a new, unknown dependence. The obtained constrained modulus  $M_{DMT}$  was compared with cone resistance  $q_c$  to determine the relationship between them. As a result a formula in the form of a simple mathematical equation was determined, which on the basis on the results of static probe (CPT) allows the prediction of the com-

pressibility of the soil expressed by the constrained dilatometric modulus  $M_{DMTp} \approx 14 \cdot q_c$ ,

where:  $M_{DMTp}$  – predicted constrained dilatometric modulus,

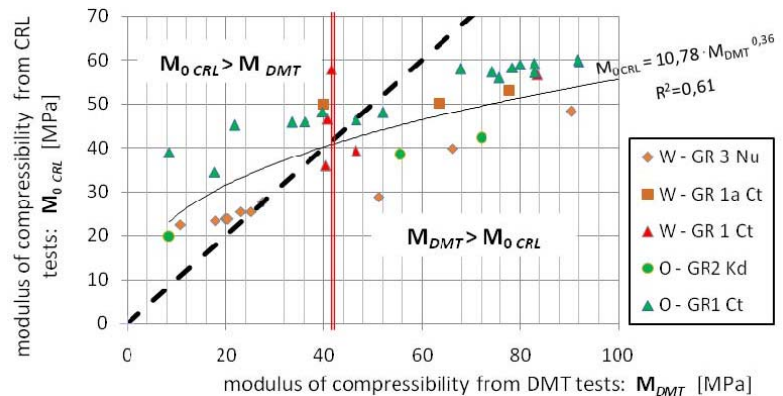
$q_c$  – cone resistance CPT(u)

Detailed results from **Nu** and **Ct** sites are shown in Text-fig. 16. The graph does not include the results from **Kd** site. This is due to the spatial variability of the soil. Since the distance between the probes CPT and DMT was approx. 30 m, there were no significant relationship between the parameters under consideration.

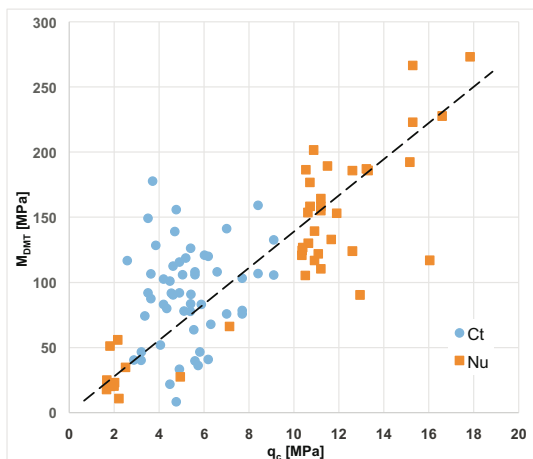
### Evaluation of compression state

The changes in the characteristics of the soil compressibility in a function of stress depend on many factors generally associated with structural changes and load history (Text-fig. 17).

The magnitude of consolidation is expressed by the yield  $\sigma'_{vy}$  (or preconsolidation  $\sigma'_p$ ) (Burland 1990; Szczepeński 2007). On the basis of on the yield stress, yield stress ratio may be calculated expressed as YSR



Text-fig. 15. Character of dependence between compressibility modulus obtained from dilatometer DMT and consolidometer CRL tests



Text-fig. 16. Correlation between  $q_c$  and  $M_{DMT}$  in field tests (CPT(u) and DMT)

$= \sigma'_{vy} / \sigma'_0$  (which equals OCR value in classical terminology). It constitutes as an important indicator of soil behaviour in many other studies.

In order to determine these values properly, laboratory testing of compressibility were conducted under a stress range that significantly exceeds the yield stress. In this case the choice of loading method (IL or CL) was less important. Most often such a stress range is not possible to achieve using standard laboratory equipment. In practice, oedometers are widely used with a maximum load capacity of 1.6 or 3.2 MPa. Such a stress range prevents the obtaining of reliable results of yield  $\sigma'_{vy}$  in the case of strongly consolidated soils. In geological contexts preliminary analysis of the geological history of soil, together with the estimated historical load of a glacier and overlying soil indicates the necessity of involving in the research such instruments that allow to the load

testing of material up to a much larger values. The analysis of the results of 20 tests on tills was carried out both in the range of loads generated in standard laboratories (about 2 MPa) and for a much extended range of loads (20 MPa).

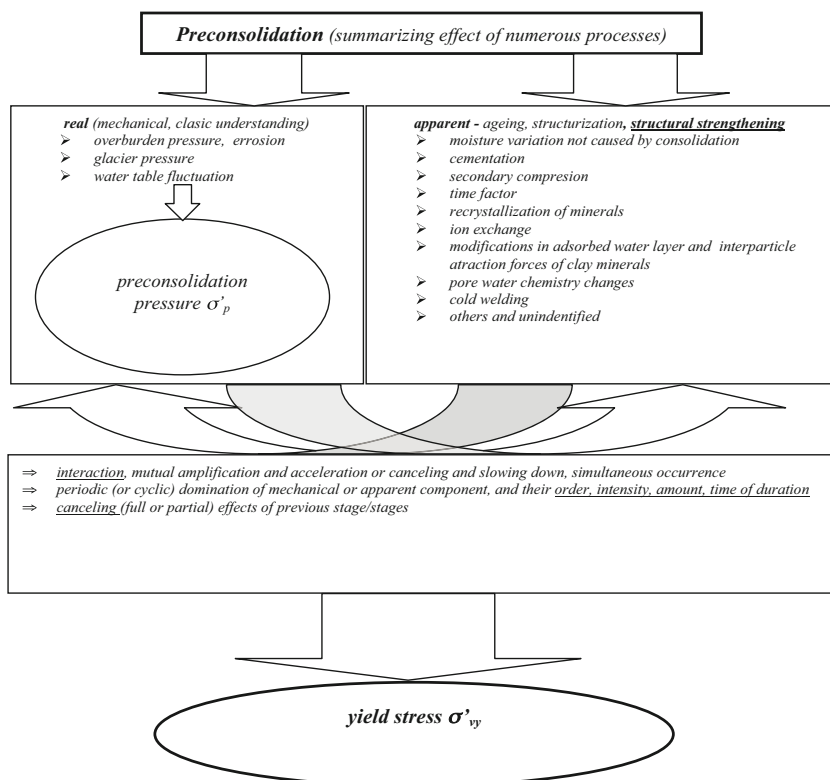
The other important reasons for the discrepancies of preconsolidation analysis are associated with different methods of the yield stress  $\sigma'_{vy}$  (or preconsolidation  $\sigma'_p$ ) determination (Szczepański 2007). A multitude methods firstly demonstrates how important is to determine the correct  $\sigma'_p$ , and secondly shows how difficult it is. The most common and most frequently used method (despite its imperfections) is a graphical method developed by Casagrande (1936). Its main disadvantage is a certain subjectivity in choosing the point of maximum deflection of compressibility curve. For that reason, in the presented analysis the method proposed by Becker *et al.* (1987) was used instead of the Casagrande method. The method was verified for the purposes of CRL tests by Szczepański (2005) and is based on the criterion of work per volume unit. In this article this method is called “W” method.

An example of compressibility curve in two stress ranges up to 2 and up to 20 MPa, together with the interpretation by Cassagrande method and “W” method is given in Text-fig. 18.

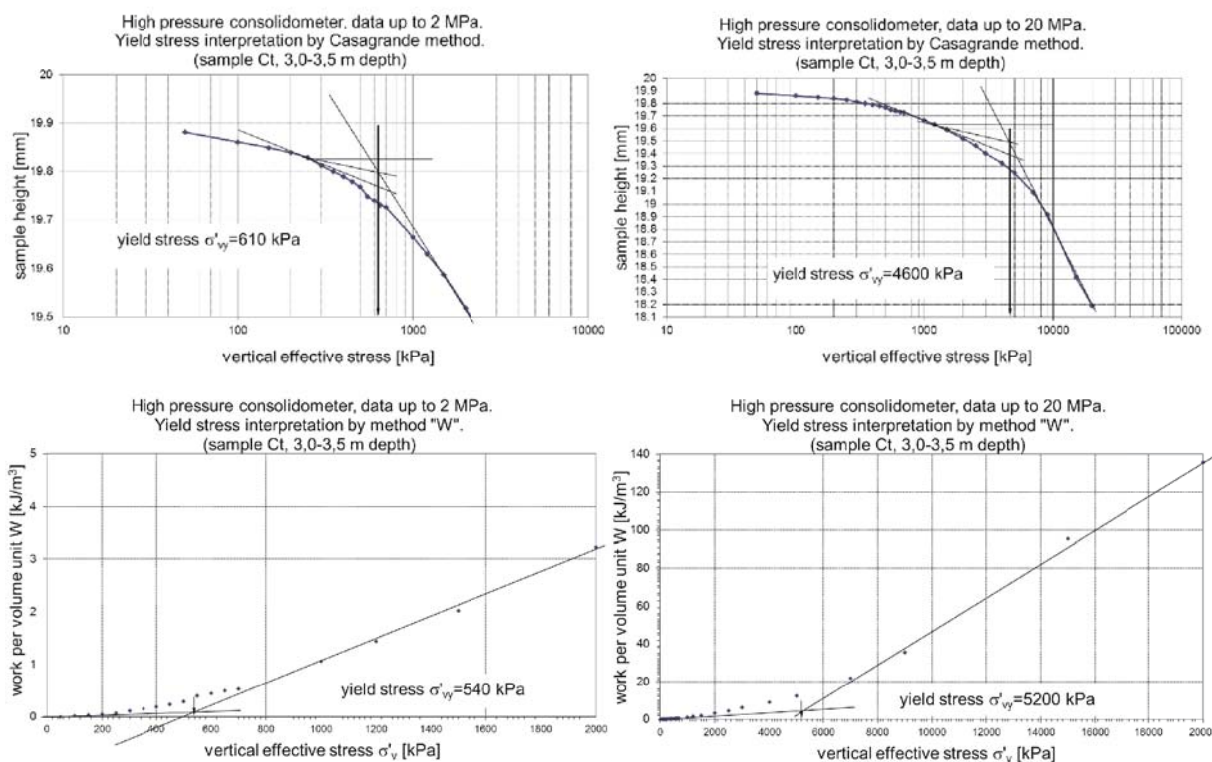
After interpretation of the studies it was concluded that, depending on the extent of the analyzed loads, two yield points are obtained – the first of several hundred and the second of several thousand. However, one issue still remains open – the physical meaning of these two values in terms of the compressibility characteristics of one soil type.

On the basis of such comparisons it should be questioned if the method of interpretation used was correct. According to the previously performed analyses (Szczepański 2005), the “W” method at low ranges

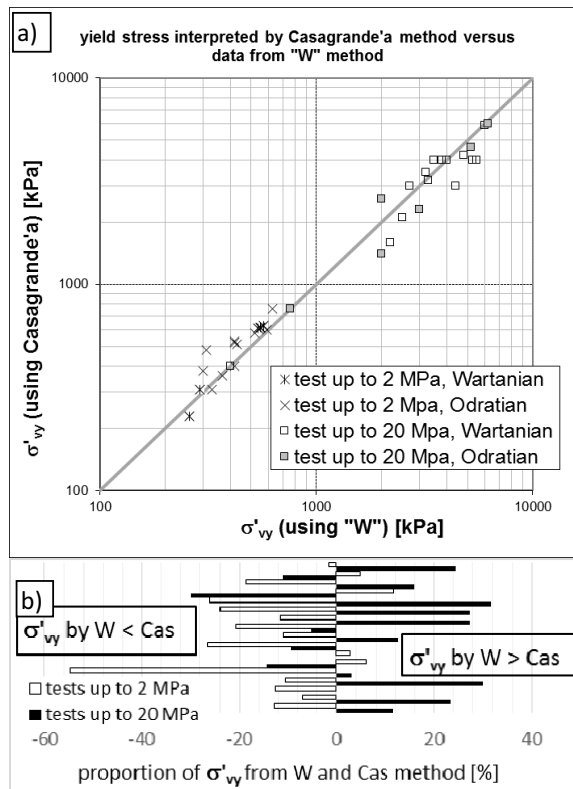




Text-fig. 17. Factors affecting the preconsolidation phenomenon and their connection with the output parameter – yield stress



Text-fig. 18. Example of compressibility test with yield stress interpreted within two stress ranges (2 and 20 MPa – left and right graphs respectively) using two methods (classic Casagrande method, and so called “W” method (Becker *et al.* 1987) – upper and lower graphs respectively)

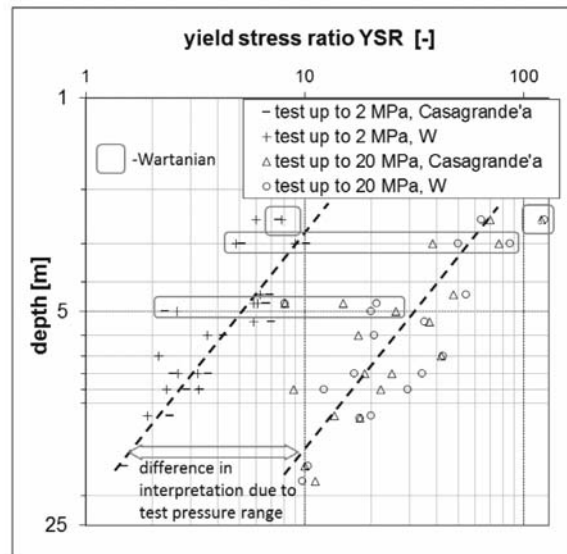


Text-fig. 19. a. Yield stress interpreted within two stress ranges (2 and 20MPa) with use two methods (classic Casagrande method, and so called "W" method (Becker *et al.* 1987)); b. Relative proportion between yield stress obtained from both methods

is less subjective than classic Cassagrande method as it produces lower dispersion of the results. However, according to the current study, concordance of the results obtained from both methods was observed (Text-fig. 19), although some exceptions occur. This may provide a confirmation that both methods were correct. There was however an interesting relationship referring to the relatively higher values obtained in the Casagrande method at a low stress range and the inverse interpretation at stress up to 20 MPa.

The summary relationships between the results of the aforementioned methods is illustrated in Text-fig. 20. In case of the first yield point, a tendency to overestimate the value by Cassagrande method was observed. In case of the second yield point, the "W" method brought higher values. No influences of litho stratigraphic position on the obtained results was noticed. The variety of the estimations at the first yield point is clearly higher and is associated with the greater uncertainty at lower stresses.

There is a clear relationship of YSR in the function of depth from which the samples were taken. It is ex-



Text-fig. 20. Yield stress ratio YSR calculated for yield stresses resulted from two interpretation stress ranges and two interpretation methods

pressed in quasi parallel approximation lines of YSR points illustrating not only the difference in interpretation due to test pressure range but also due to the rate of decrease in the value of YSR with depth of the soil sampling.

Extremely high values of yield stress (and the yield degree) in some cases may be surprising, but it should be remembered that the traditional opinions on the direct correspondence between yield stress and the historical load do not fit to the current knowledge on this subject. It is widely known, that there are many factors imposing themselves and enhancing or eliminating the historical load influence (Text-fig. 17). This results in the effect of apparent preconsolidation (structural reinforcement) on a completely different level than would result from specific preconsolidation stress. In addition the hypothesis that the second yield point may be affected by grains crushing under high loads was considered but it was not confirmed in microstructural studies in different scales (Kaczyński *et al.* 2008a). Studies were carried out both on the samples before and after the load application but the results did not provide any support for this hypothesis.

### Permeability assessment

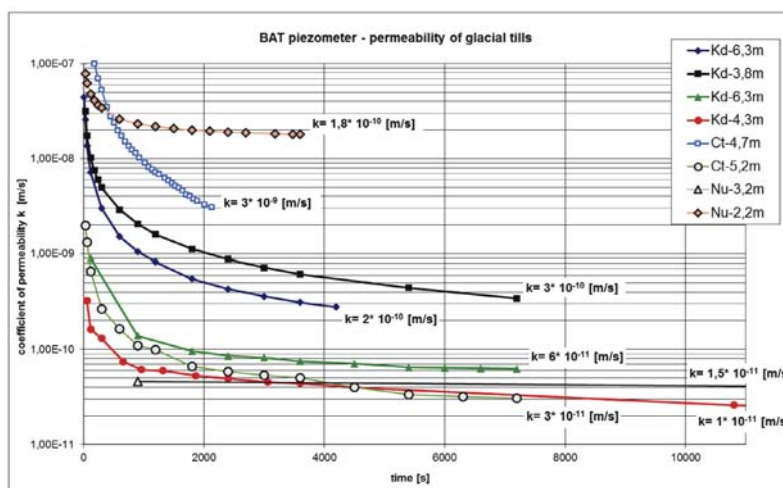
The permeability assessment of tested tills was carried out using BAT field method together with the interpretation of laboratory consolidation tests of the CRL type.

A field test of permeability by the BAT system showed a large variation in the value of the permeability coefficient “k” (see Text-fig. 21). The greater variability of the permeability coefficient for Wartanian tills may be a result of the variability in lithology. For the same reason Odranian tills are characterized by a smaller permeability coefficient as they have more clay fraction.

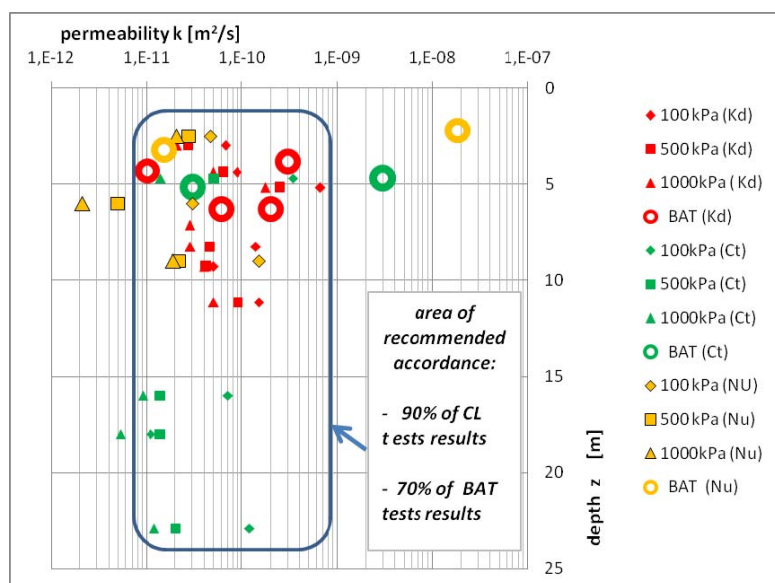
In laboratory CRL tests, all till samples taken from a depth of 2.5 to 23 m below the surface were subjected to loads with a constant speed of about 30 kPa/h until the value of  $\sigma$  reached about 1800 kPa. This wide range of loads led to the obtaining of the typical course of CL characteristics of parameters (compressibility modulus, consolidation coefficient and perme-

ability coefficient calculated on the basis of the first two parameters) in a function of stress. In case of permeability analysis, at first high values of this parameter are obtained. Then, at the initial stage of testing, the values decrease quickly later on showing a quasi-rectilinear, slow decrease correlated with the so-called stable state of the test. To consider this variability in comparative analyses of the results obtained from the BAT and CRL method only k values obtained at stress of 100 kPa, 500 kPa and 1000 kPa were selected.

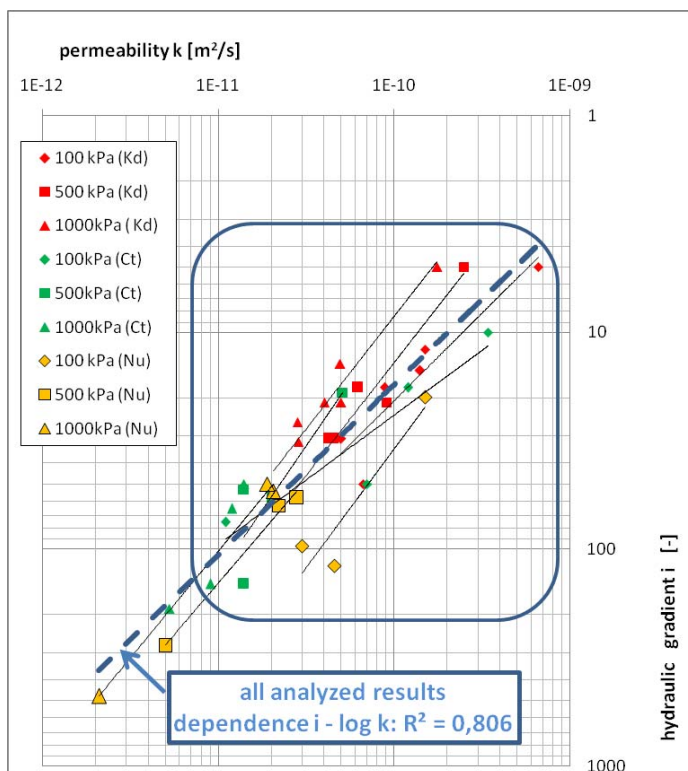
During evaluation of the results, it must be taken into account that the k coefficient, especially in case of poorly permeable soils, is a parameter with a significant variability. It is expressed in one or two orders of magnitude difference while comparing the results of



Text-fig. 21. Results of BAT piezometer measurements



Text-fig. 22. Permeability coefficient values in the background of depth of soil (data obtained from BAT and CL tests)

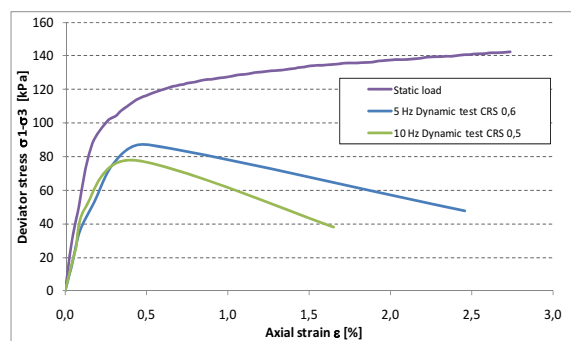


Text-fig. 23. Dependence between permeability coefficient versus hydraulic gradient obtained from CL tests (data under selected stress)

different testing methods and different constraint conditions (Kaczyński 2000).

As stated above, lithology and soil saturation (in fact conductivity of the liquid phase of pore space) are the main factors causing the variability of  $k$  values. The saturation of tested soil samples was 0.95 – 0.99. These are typical values for overconsolidated soils. This of course affects the relatively low values of pore pressure. Despite the difficulties in mobilization of pore pressure in the consolidated structure of the solid phase, consolidation-permeability parameters were comparable with literature data. Comparison shown in Text-fig. 22 proves that 90% and 70% of analysed  $k$  values from CRL and BAT tests respec-

tively, were within the range of  $k$  from  $10^{-9}$  to  $10^{-11}$  m/s. This indicates a generally good concordance of these two methods. A small number of lower  $k$ -values is connected with high stresses in the consolidometer not comparable to those under natural conditions whereas several higher  $k$ -values obtained from BAT may be associated with the occurrence of more permeable layers. It should be underlined that a tendency of  $k$ -values to decrease was noticed in the soil sampled at deeper parts of the profile. This may result from the smaller impact of exogenous factors in the deeper part of the profile and a smaller soil relaxation. Analysis of the results of consolidometer tests allowed the assessment of the impact of the hydraulic gradient occurring in a consolidated sample due to the mobilization of pore pressure on the obtained values of the permeability coefficient. The water pressure in the pore space induces not only a source field of seepage, but also specific effects of its choking, rising together with a pore pressure. The relation between permeability coefficient and hydraulic gradient can be treated as an indicator of their relationship. The studies brought out quite a clear trend, described as a power function. Based on all the analyzed results a relatively good correlation between hydraulic gradient  $i$  and permeability  $k$  was obtained, which is also compliant with  $i - k$  lines (Text see fig. 23) at the following stress values: 100, 500 and 1000 kPa.



Text-fig. 24. Comparison graph of deviator stress changes resulting from triaxial tests using static and dynamic loading of frequency of 5–10 Hz

| Glaciation | Dynamic test type          | Test type  | Deviator stress at failure [kPa] | Shear strength reduction $\tau_c/\tau_s$ [%] |
|------------|----------------------------|--|----------------------------------|--|
| Wartanian  | Axial displacement control | Static load  | 152                              | -  |
|            |                            | 10 Hz Dynamic test - 0.1 mm displacement amplitude | 100                              | 65   |
|            |                            | 10 Hz Dynamic test - 0.4 mm displacement amplitude | 72                               | 47   |
| Odranian   | Load control dynamic       | Static load  | 142                              | -  |
|            |                            | 5 Hz Dynamic test CRS 0.6                          | 87                               | 61   |
|            |                            | 10 Hz Dynamic test CRS 0.5                         | 78                               | 54   |

Table 7. Reduction of shear strength of tills on the basis of triaxial test results

### Shear strength of soils under dynamic loading

The strength characteristics of the samples of Wartanian tills was determined in static tests preceded by a stage of dynamic loading under axial displacement control conditions. During dynamic loading, no failure was observed. However, the results obtained in post-cyclic shearing (Table 7) indicate the shear strength reduction. The post-cyclic shear strength ranged from 47 to 65% of the static strength of soils which were not subjected previously to dynamic loads. Strength reduction is greater in case of a higher vibration amplitude.

During the dynamic test conducted under load control conditions (Text-fig. 24) the strains of the samples are the biggest at the first cycle of loading, whereas strain increments decrease together with the increase of the number of cycles. This happens until the moment of limit stress (load) value is reached and the soil structure is weakened together with an increase of pore pressure. If the stress does not exceed the limit value deformations and pore pressure stabilizes at a constant level. At steady-state conditions, each following loop will overlap the former one creating so-called stabilized hysteresis loop. The number of cycles needed to reach a steady state was determined experimentally and it was determined as more than 3000 cycles. The following peaks of hysteresis loop for various load ranges define a cyclic stress-strain curve.

The reduction of the shear strength of the Odranian tills ranged from 61 to 51%, whereas a loss of shear strength rises together with increasing frequency of dynamic loads. The extent of the strain accompanying the failure of the samples under dynamic loading depends on the frequency of vibration applied – the higher the frequency is, the less strain is observed at the time of failure.

### CONCLUSIONS

1. The analysis of the lithogenetic characteristics, selected properties and of the mechanical behavior of the studied tills indicates at least three possible determinants of their variability: (1) conditions of soil deposition, (2) stratigraphic position, and (3) post-sedimentary transformation associated with weathering and stress relaxation in soil profiles. These factors are variably reflected in the formation of physical and mechanical properties of a soil of glacial origin.
2. The effects of conditions of soil deposition illustrates the differences between the analyzed lithological profiles. The nature of the soil variability in the Ct profile is because of the manner of deglaciation by the melting of dead ice blocks stagnant in the depressions. In turn, the macro, meso- and microstructural properties of the till from the Nu and Kd sites classify the studied tills into the group of the so-called lodgement tills (where material from the lower part of the glacier was deposited directly under the moving glacier).
3. The expected differences in the properties of the Wartanian and Odranian tills appear macroscopically (color, the content of the sand fraction) and in the microstructural analysis. A slightly higher number of the micro pores, the fissure pores and higher microstructure anisotropy is noticed. The dynamics observed from the ice-sheet movement and deglaciation can also involve changes in the degree of compaction and separation surfaces underlined by the ferrous traces. The analysis of microstructures for land taken in its natural state and after the one-dimensional compressibility tests indicates that the in-

crease of degree of compaction of structural elements and the decrease in the porosity are more substantial in samples tested under a slower rate of load. The variability of selected indicators of the mineral composition (the content of the clay fraction, carbonates, and the ratio of the goethite to siderite) shows both the stratigraphic conditions and differences in intensities of post-sedimentary exogenous processes.

4. The assessment of the impact of load history on the mechanical properties of the tills needed to be expanded to 20 MPa of stress range in the compressibility tests. This made it possible to distinguish two yield points obtained respectively at the values of several hundred and several thousand MPa. This indicates the complexity of soil deformability and the limited reliability of overconsolidation assessed traditionally in low ranges of stress. An alternative method of determining the yield stress demonstrated that in the first (lower) yield point of the compressibility graph, yield stresses are more variable and higher than using the Cassagrande's method. On the other hand, the newer "W" method gives a higher stress estimation in the second yield point. Conducted alternative tests document the ranges of variation of yield stress. It allows the assessment of the accuracy of historical loads on the basis of deformability tests.
5. Comparison of the values of selected field and laboratory parameters indicates limited possibilities of correlation. Low permeability of  $10^{-9}$ – $10^{-11}$  m/s was obtained under both BAT and consolidometer tests. A clear trend of reducing the permeability coefficient with increasing hydraulic gradient in consolidometer tests suggests flow contraction with pore water pressure increase in poorly permeable soil. This may affect the assessment of insulating properties and elongation of consolidation.
6. The overconsolidated tills studied are not very compressible. This results in a weak correlation between the constrained modules obtained from dilatometer  $M_{DMT}$  and consolidometer  $M_0$ , and also between cone resistance  $q_c$  and constrained dilatometric modulus  $M_{DMT}$ . When  $M_{DMT} < 40$  MPa  $M_0$  values for samples taken from the same locations are higher. Generally, the characteristics of  $M_{DMT}$  are more selective which allows the assessment of the variability of the soil profile and the safer prediction of deformation of a subsoil.

7. Dynamic loading can be another factor weakening the structure of overconsolidated soils. Wartanian and Odranian tills show 'clay-like' behavior (Boulanger and Idriss 2004, 2006) under dynamic loading pore pressure reaches a high constant value, but less than the total stress (effective stress  $\neq 0$ ) and due to the decrease of effective stress a significant weakening occurs. The test results show that dynamic loading causes a shear strength reduction. Dynamic shear strength ranges from 47 to 65% of the static shear strength. The shear strength reduction is related not only to a reduction of effective stress due to the increased pore pressure, but also to change of soil structure during dynamic loading (Bąkowska 2009). Dynamic and post-dynamic (post-cyclic) shear strength of cohesive soils depends on the intensity of the applied vibration (amplitude and frequency of the load, the number of applied load cycles) and the test type.
8. The applied program of advanced geological-engineering studies indicates that the variability of structural and mechanical properties of soil is determined by natural and anthropogenic factors. The role of natural factors depends on the geological-structural and exogenous transformation of the upper part of the soil profile. The nature and size of loading which affect the soil profile today due to the existence of buildings and infrastructure may affect the variation of the subsoil response much more than the relatively homogeneous characteristics of Middle Polish glaciations tills.

## REFERENCES

- ASTM D 2487-98. Standard Practice for Classification of Soils for Engineering Purposes (Unified Soil Classification System). American Society for Testing and Materials, Philadelphia, pp. 238–247.
- ASTM D 5298-94. Standard test methods for measurement of soil potential (suction) using filter paper. American Society for Testing and Materials, Philadelphia, pp. 1082–1087.
- Bąkowska, A. 2009. Zachowanie się glin lodowcowych rejonu Warszawa-Służew pod wpływem obciążeń dynamicznych. Praca doktorska, Uniwersytet Warszawski, Warszawa. Archiwum WG UW, pp. 52–93.
- Bąkowska, A., Kiełbasiński, K. and Zawrzykraj, P. 2010. Physical and mechanical properties of tills from Służew area in Warsaw in the light of in situ tests. In: Soil parameters from in situ and laboratory tests, pp. 159–168, Poznań University of Life Sciences; Polish Committee on Geotechnics.

- Becker, D.E., Crooks, J.H.A., Been, K. and Jefferies, M.G. 1987. Work as a criterion for determining in situ and yield stresses in clays. *Canadian Geotechnical Journal*, **24**, 549–564.
- Boulanger, R.W. and Idriss, I.M. 2004. Evaluating the potential for liquefaction or cyclic failure of silts and clays. Center for Geotechnical Modeling, Raport No. UCD/CGM-04/01, Department of Civil and Environmental Engineering, College of Engineering, University of California; Davis, pp. 54–78.
- Boulanger, R.W. and Idriss, I.M. 2006. Liquefaction susceptibility of criteria for silts and clays. *Journal of Geotechnical and Geoenvironmental Engineering*, ASCE, **132**, 1413–1426.
- Boulton, G.S. 1972. Modern Arctic glaciers as depositional models for former ice sheets. *The Journal of the Geological Society*, **128**, 361–393.
- Boulton, G.S. 1976. A genetic classification of tills and criteria for distinguishing tills of different origin. In: W. Stankowski (Eds), Till, its genesis and diagenesis. *Zeszyty Naukowe UAM*, Geografia, **12**, 65–80.
- Brodzikowski, K. and Van Loon, A.J. 1991. Glacigenic sediments. *Developments in sedimentology*, 49, 674 p. Elsevier; Amsterdam.
- Burland, J.B. 1990. On the compressibility and shear strength of natural clays. *Géotechnique* **40**, 329–378.
- Casagrande, A. 1936. The determination of the pre-consolidation load and its practical significance. Proceedings, First International Conference on Soil Mechanics and Foundation Engineering, Cambridge, **3**, 60–64.
- Dobak, P. 1984. Problems of evaluation of the soil homogeneity based on variability of some geotechnical parameters. *Scientific Papers of the Institute of Geotechnics of Wrocław Technical University*, 44, Conferences No 17 pp 23–30.
- Dreimanis, A. 1989. Tills: Their genetic terminology and classification. In: R.P. Goldthwait, C.L. Matsch (Eds), Genetic classification of glacigenic deposit, pp. 17–81. Final Report of The Commission on Genesis and Lithology of Glacial Quaternary Deposits of The International Union for Quaternary Research (INQUA). A.A. Balkema; Rotterdam, Brookfield.
- Frankowski, Z. and Wysokiński, L. 2000. Atlas geologiczno-inżynierski Warszawy. Archiwum CAG, Warszawa, 80 p., 26 figs.
- Grabowska-Olszewska, B. (Eds) 1998. *Geologia stosowana. Właściwości gruntów nienasyconych*. PWN. Warszawa, 218 p.
- Grabowska-Olszewska, B., Osipov, V.I. and Sokolov, V.N. 1984. Atlas of the microstructure of clay soil, 414 p. Państwowe Wydawnictwo Naukowe; Warszawa.
- Gratchev, I. B., Sassa, K., Osipov, V. I. and Sokolov, V. N. 2006. The liquefaction of clayey soils under cyclic loading. *Engineering Geology*, **86**, 70–84.
- Green, R.A. and Terri, G.A. 2005. Number of Equivalent Cycles Concept for Liquefaction Evaluations – Revisited, *ASCE Journal of Geotechnical and Geoenvironmental Engineering*, **131**, 477–488.
- Hart, J.K. and Boulton, G.S. 1991. The interrelation of glaciotectionic and glaciodepositional processes within the glacial environment. *Quaternary Science Reviews*, **10**, 335–350.
- Hart, J.K. 1998. The deforming bed / debris-rich basal ice continuum and its implications for the formation of glacial landforms (flutes) and sediments (melt-out till). *Quaternary Science Reviews*, **17**, 737–754.
- Head, K. H. 1992. Manual of Soil Laboratory Testing, Vol. 1: Soil Classification and Compaction Tests, 388 p. Pentech Press; London.
- Head, K. H. 1994. Manual of Soil Laboratory Testing, Vol. 2: Permeability, Shear Strength and Compressibility Tests, pp. 335–747. Pentech Press; London.
- Izdebska-Mucha, D. and Wójcik, E. 2015. Evaluation of expansivity of Neogene clays and glacial tills from central Poland on the basis of suction tests. *Geological Quarterly*, **59**, 593–602.
- Kaczmarek, Ł. and Dobak, P. 2015. Stability conditions of the Vistula Valley attained by a multivariate approach – a case study from the Warsaw Southern Ring Road. *Geologos* **21**, 249–260.
- Kaczyński, R. and Trzciniński, J. 1997. Ilościowa analiza mikrostrukturalna w skaningowym mikroskopie elektronowym (SEM) typowych gruntów Polski. *Przegląd Geologiczny*, **45**, 721–726.
- Kaczyński, R. (Eds) 2000. Współczynnik filtracji gruntów spoistych wyznaczony różnymi metodami. [In:] Aktualne problemy geologiczno-inżynierskich badań podłoża budowlanego i zagospodarowania terenu. Bogucki Wyd. Naukowe. S.C. Poznań, pp. 57–65.
- Kaczyński, R., Barański, M., Bąkowska, A., Borowczyk, M., Gawriuczenkow, I., Kiełbasiński, K., Krauzlis, K., Laskowski, K., Pietrzykowski, P., Szczepański, T., Trzciniński, J., Wójcik, E. and Zawrzykraj, P. 2008a. Stan skonsolidowania i mikrostruktury glin zlodowacenia środkowopolskiego rejonu Warszawa-Służew na tle ich geologiczno-inżynierskich właściwości. Projekt badawczy KBN Nr 4 T12B 062 28. Archiwum NCN, 161 p.
- Kaczyński, R., Bąkowska, A. and Kiełbasiński, K., 2008b. Analiza stateczności zbocza w rejonie kościoła św. Katarzyny w Warszawie z uwzględnieniem obciążeń dynamicznych. *Acta Scientiarum Polonorum, Architectura*, **7**, 27–37.
- Kaczyński, R., Bąkowska, A. and Kiełbasiński, K. 2012. Geologiczno-inżynierska ocena statycznego i dynamicznego zachowania się gruntów występujących w przekroju doliny Wisły w Warszawie na wysokości

- Mokotów-Ursynów. Projekt badawczy N N525 362937. Archiwum NCN, 212 p.
- Kondracki, J. 1998. Geografia regionalna Polski, 441 p. PWN; Warszawa.
- Kościówko, H. and Wyrwicki, R. 1996. Metodyka badań kopalni ilastych, pp. 56–76. Państwowy Instytut Geologiczny; Warszawa.
- Krogulec, E. 1992. Określenie wartości współczynnika filtracji osadów słaboprzepuszczalnych przy zastosowaniu systemu monitoringu wód podziemnych BAT. *Technika Poszukiwań Geologicznych*, **5**, 47–51.
- Krogulec, E. 1997. Numeryczna analiza struktury strumienia filtracji w strefie krawędziowej poziomo błońskiego (kotliny Warszawskiej). Praca doktorska, 78 p. Wydawnictwa Uniwersytetu Warszawskiego; Warszawa.
- Lawson, D.E. 1997. Sedimentological analysis of the western terminus region of the Matanuska Glacier, Alaska. Cold Region Research and Engineering Laboratory. Report **79**, 1–112.
- Lee, I.K., White, W. and Ingles, O.G. 1983. Geotechnical engineering, 508 p. K. Pitman; Massach.,
- Lunne, T., Robertson P.K. and Powell J.J.M. 1997. Cone Penetration Testing in geotechnical practice. Blackie Academic and Professional; London.
- Marchetti, S. 1980. In situ tests by flat dilatometer. *Journal of the Geotechnical Engineering Division*, ASCE, **106**, 299–321.
- McKeen, R.G., 1992. A Model for Predicting Expansive Soil Behavior. Proceedings of the 7th International Conference on Expansive Soils, Dallas, 1, 1–6.
- Młynarek, Z. and Wierzbicki J. 2007. Nowe możliwości i problemy interpretacyjne połowych badań gruntów. W: Współczesne problemy geologii inżynierskiej w Polsce. *Geologos*, **11**, 97–118.
- Myślińska, E. 2006. Laboratoryjne badania gruntów, 278 p. UW; Warszawa.
- Osipov, V.I. 1979. Nature of strength and deformation properties of clay soils, 235 p. Publishing House of the Moscow State University; Moscow. [In Russian]
- Osipov, V. I., Nikolaeva, S. K. and Sokolov, V. N. 1984. Microstructural changes associated with thixotropic phenomena in clay soils. *Géotechnique*, **34**, 293–303.
- Osipov, V.I., Sokolov V.N. and Rumyanцева N.A. 1989. The microstructure of clay soils, 211 p. Nedra; Moscow. [In Russian]
- Petsonk, A., Romanowski, W. and Richards, V. 1989. Field permeability testing for RCRA landfill final cover, USA. Proceedings of Hazmacon '87, Santa Clara, California April 22, 1987, 12 p.
- Pinińska, J. and Dobak, P. 1987. Zmienność parametrów geotechnicznych w warunkach budowy metra w Warszawie. *Przegląd Geologiczny*, **2**, 73–79.
- Piotrowski, J.A. Doring, U., Harder, A., Qadirie, R. and Wenghofer, S. 1997. Deforming bed conditions on the Danischer Wohld Peninsula, north Germany: Comments. *Boreas*, **26**, 73–77.
- PN-88/B-04481 – Grunty budowlane, badania próbek, 45 p.
- PN-B-02481. Geotechnika. Terminologia podstawowa, symbole literowe i jednostki miar, 27 p.
- Ruszczyńska-Szenajch, H. 1983. Lodgement tills and syn-depositional glaciotectionic processes. Related to subglacial thermal and hydrologic conditions. In: E.B. Evenson, Ch. Schluchter and J. Rabassa (Eds), Tills and related deposits. Proc. of the INQUA Symposia on the Genesis and Lithology of Quaternary Deposits /USA 1981/Argentina 1982, pp. 113–117. A.A. Balkema; Rotterdam.
- Ruszczyńska-Szenajch, H. 1998. Struktura glin lodowcowych jako istotny wskaźnik ich genezy. In: E. Mycielska-Dowgiałło (Eds), Struktury sedimentacyjne i postsedimentacyjne w osadach czwartorzędowych i ich znaczenie diagnostyczne, pp. 13–43. Uniwersytet Warszawski, Warszawa.
- Ruszczyńska-Szenajch, H., Trzciniński, J. and Jarosińska, U. 2003. Lodgement till deposition and deformation investigated by macroscopic observation, thin section analysis, and electron microscope study. *Boreas*, **32**, 399–415.
- Sergeev, Y.M., Osipov, V.I. and Sokolov, V.N. 1985. Quantitative analysis of soil structure with the microcomputer system. *Bulletin of the International Association of Engineering Geology*, **31**, 131–136.
- Sergeev, Y.M., Spivak, G.V., Sasov, A.Y., Osipov, V.I., Sokolov, V.N. and Rau, E.I. 1984. Quantitative morphological analysis in a SEM-microcomputer system – I, II. *Journal of Microscopy*, **135**, 1–24.
- Sergeyev, Y. M., Grabowska-Olszewska, B., Osipov, V. I. and Sokolov, V. N. 1978. Types of the microstructures of clayey soils: Proceedings of the III International Congress I.A.E.G., **1**, 319–327.
- Sergeyev, Y. M., Grabowska-Olszewska, B., Osipov, V. I. and Sokolov V. N. and Kolomenski Y. N. 1980. The classification of microstructures of clay soil. *Journal of Microscopy*, **120**, 237–260.
- Shaw, J. 1977. Till body morphology and structure related to glacier flow. *Boreas*, **6**, 189–201.
- Shi, B., WU, Z., Inyang, H., Chen, J. and Wang, B. 1999. Preparation of soil specimens for SEM analysis using freeze-cut-drying. *Bulletin of Engineering Geology and the Environment*, **58**, 1–7.
- Sikora, Z. 2006. Sondowanie statyczne. Metody i zastosowanie w geoinżynierii, 350 p. Wydawnictwo Naukowo-Techniczne; Warszawa.
- Smart, P. and Tovey, K. 1982. Electronmicroscopy of soils and sediments: techniques, 264 p. Clarendon Press; Oxford.



- Sobolewski, M. and Bajda, M. 2001. Wpływ uwilgotnienia gruntu na zmianę jego właściwości filtracyjnych. I Krajowa Konferencja Młodych Geotechników „Rozwój badań i modelowanie w geotechnice”. Przegląd Naukowy Wydziału Inżynierii i Kształtowania Środowiska, **20**, 89–98.
- Sokolov, V. N., Yurkovets, D. I. and Razgulina, O. V. 2002. Stiman (Structural Image analysis): a software for quantitative morphological analysis of structures by their images (User's manual. Version 2.0), 75 p. Laboratory of Electron Microscopy, Moscow State University Press; Moscow.
- Sokolov, V.N. 1990. Engineering-geological classification of clay microstructures. Proceedings of 6th International IAEG Congress, Rotterdam, 753–760. A.A.Balkema.
- Szczepański, T. 2005. Ocena stanu skonsolidowania wybranych ilów na podstawie analizy parametrów ścisłości. Ph.D. Thesis, 148 p. Archiwum Wydziału Geologii UW; Warszawa.
- Szczepański, T. 2007. OCR a YSR, czyli klasyczne i współczesne poglądy na prekonsolidację gruntów ilastych. *Przegląd Geologiczny*, **55**, 405–410.
- Torstensson, B. A. 1984. A new system for ground water monitoring. *Ground Water Monitoring Review*, **4**, 131–138.
- Torstensson, B. A. and Petsonk, A. 1986. A device for in situ measurement of hydraulic conductivity. Proc. 4th International Geotechnical seminar on Field Instrumentation and in situ Measurements. Singapore, pp. 157–162.
- Tovey, N.K. and Wong K.Y. 1973. The preparation of soils and other geological materials for the S.E.M. Proceedings of the International Symposium on Soil Structures, **1**, 59–67.
- Trzcíński, J. 1998a. Ilościowa analiza mikrostrukturalna w skaningowym mikroskopie elektronowym (SEM) gruntów poddanych oddziaływaniu wody. In: B.Grabowska-Olszewska (Ed.), *Geologia stosowana. Właściwości gruntów nienasyconych*, pp. 113–150. Wydawnictwo Naukowe PWN; Warszawa.
- Trzcíński, J. 1998b. Mikrostruktury a właściwości geologiczno-inżynierskie glin lodowcowych. Ph.D. Thesis, 165 p. Archiwum Wydziału Geologii, Uniwersytet Warszawski; Warszawa.
- Trzcíński, J. 2004. Combined SEM and computerized image analysis of clay soils microstructure: technique & application. In: R.J. Jardine, D.M. Potts, and K.G. Higgins (Eds), *Advances in geotechnical engineering: The Skempton conference*, pp. 654–666. Thomas Telford; London.

*Manuscript submitted: 5<sup>th</sup> March 2016*

*Revised version accepted: 16<sup>th</sup> August 2016*